

X-ray Optics and Imaging

Ladislav Pína

Czech Technical University, Prague, Czech Republic

X-ray photonics group

- **X-ray systems R&D**

- Laboratory and space optics
- Plasma sources
- Detection techniques

- **X-ray applications**

- Capillary discharge EUV source equipped with focusing optics
- X-ray lithography
- X-ray tomography (50 - 420 kV)
- X-ray all sky monitor simulations
- Future x-ray telescopes

Cooperation

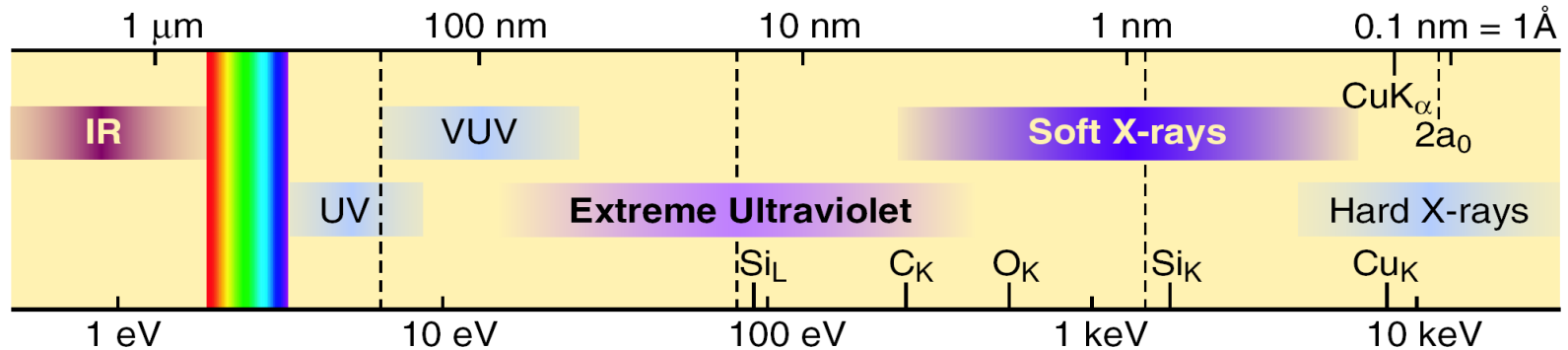
- Academy of Sciences of the Czech Rep.
- Rigaku Innovative Technologies Europe s.r.o. – hi-tech Ltd., x-ray optics, detectors, sources
- Institute of Opto-Electronics Warsaw, Poland
- Others (ESA, NASA, industry, academic institutions ...)



Spectrum of X-ray Radiation

- **EUUV (50 eV)**
- **XUV (100 eV)**
- **SXR (100 eV – 1 keV)**
- **XR (1 keV – 10 keV)**
- **HXR (100 keV)**
- **Gamma Rays (100 keV – 100 TeV)**

Electromagnetic radiation spectrum



D. T. Attwood *Soft X-rays and Extreme Ultraviolet Radiation: Principles and Applications* (Cambridge University Press, Cambridge, 1999)

13.5 nm – 92 eV

EUV Lithography

6.2 nm – 200 eV

BEUV Lithography

2.34 – 4.39 nm – 283 - 531 eV

Water Window Microscopy

Applications of X-ray Radiation

- **Medicine – radiography, tomography, therapy**
- **Industry – NDT, material research**
- **X-ray diffraction - crystallography, genetics, pharmaceutical industry**
- **EUV lithography – nanopatterning, semiconductor industry**
- **Diagnostics of hot plasmas – spectroscopy, imaging, basic research**
- **Astrophysics – stars, black holes, gamma bursts**

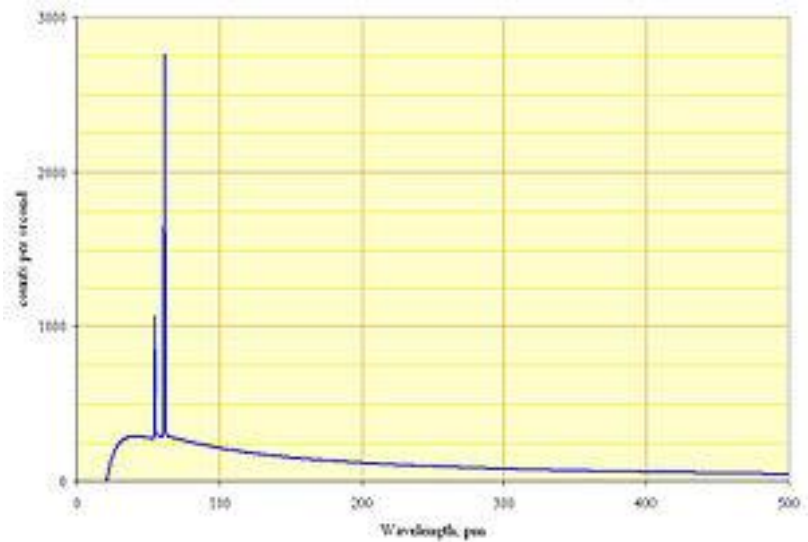
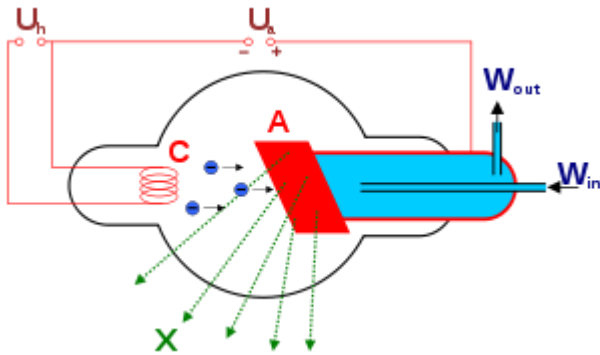
Generation of X-ray Radiation

- **Change of velocity vector of charged particle – continuum spectrum - Brehmstrahlung**
- **Change of state of quantum system – quantum transitions - line spectrum**

Typical Sources of X-ray Radiation

- **X-ray Tube (electron beam interacting with a solid target)**
- **Synchrotron**
- **Free Electron Laser**
- **Hot Plasma (Laser plasma, Tokamak, Z-pinch, Plasma focus, Stellar objects)**

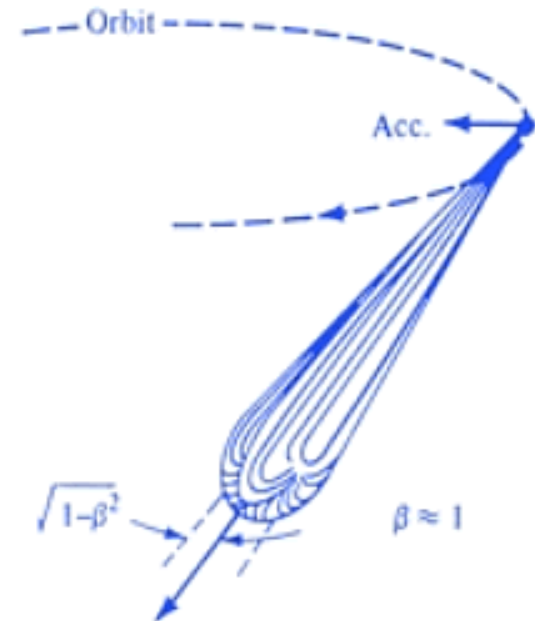
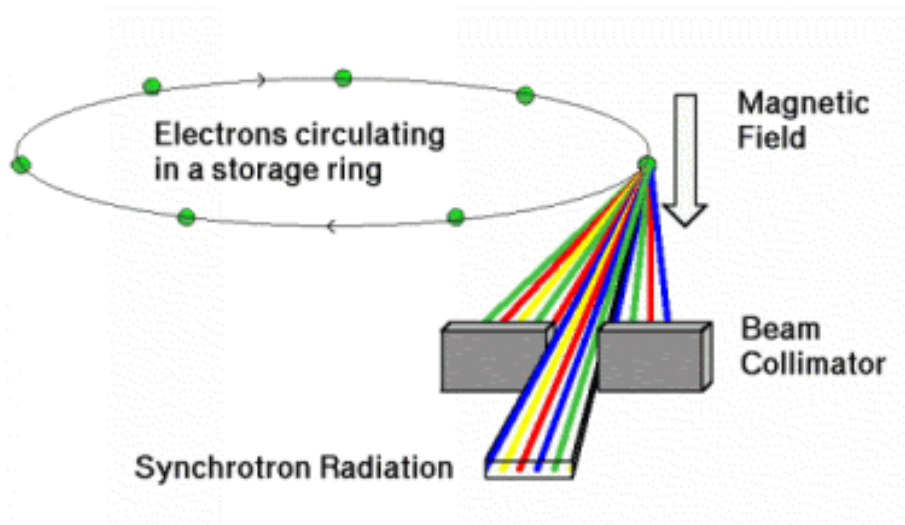
X-ray Tube



Characteristics of X-ray Tube

- Relatively low brightness
- 2π sterad diverging beam
- Wide energy spectrum: Characteristic and Bremsstrahlung (2 keV to 430 keV)
- Not polarised.
- Continual
- Microfocus
- Stable solid anode, rotating anode, liquid metal jet anode
- Coupling to XR optics possible

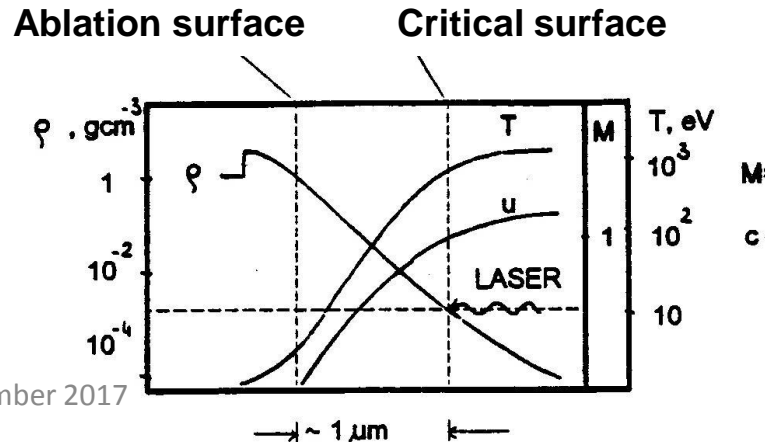
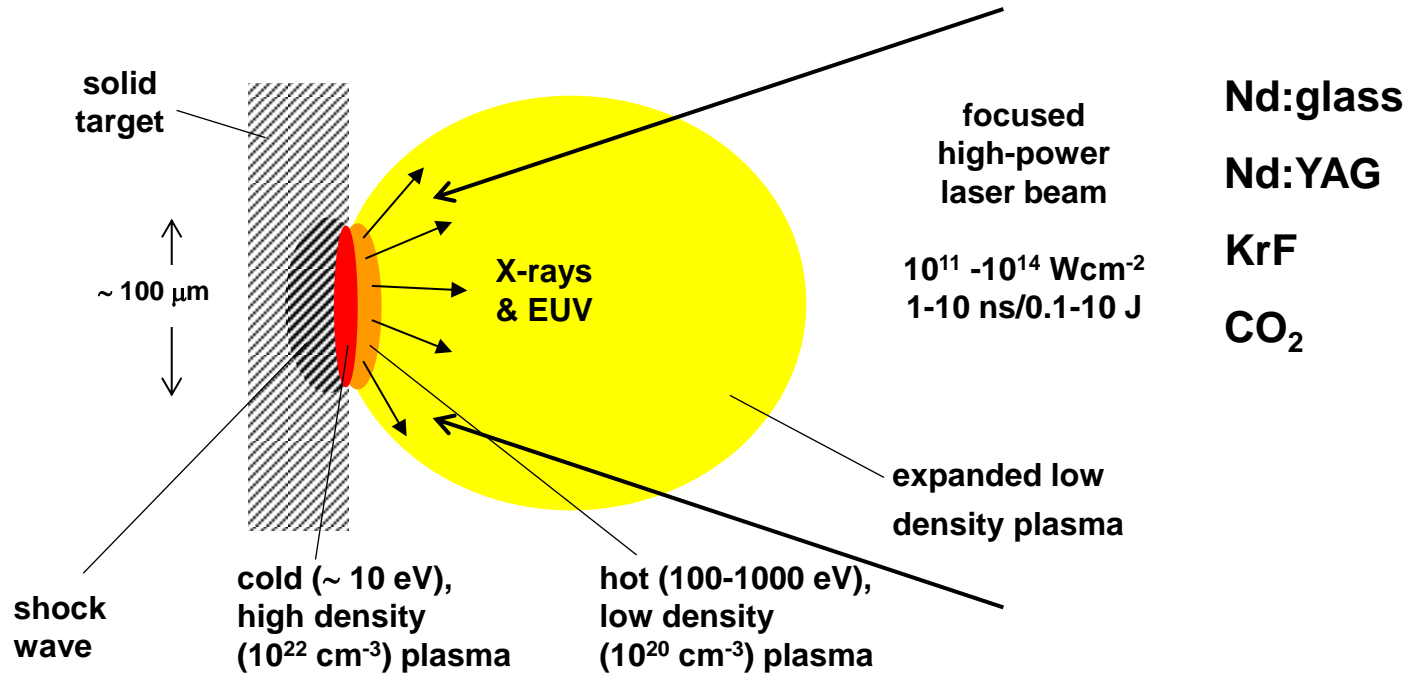
Synchrotron radiation ... >>> FEL



Characteristics of Synchrotron Radiation

- High brightness: synchrotron radiation is extremely intense (hundreds of thousands of times higher than conventional X-ray tubes) and highly collimated.
- Wide energy spectrum: synchrotron radiation is emitted with a wide range of energies, allowing a beam of any energy to be produced.
- Synchrotron radiation is highly polarised.
- It is emitted in very short pulses, typically less than a nano-second.

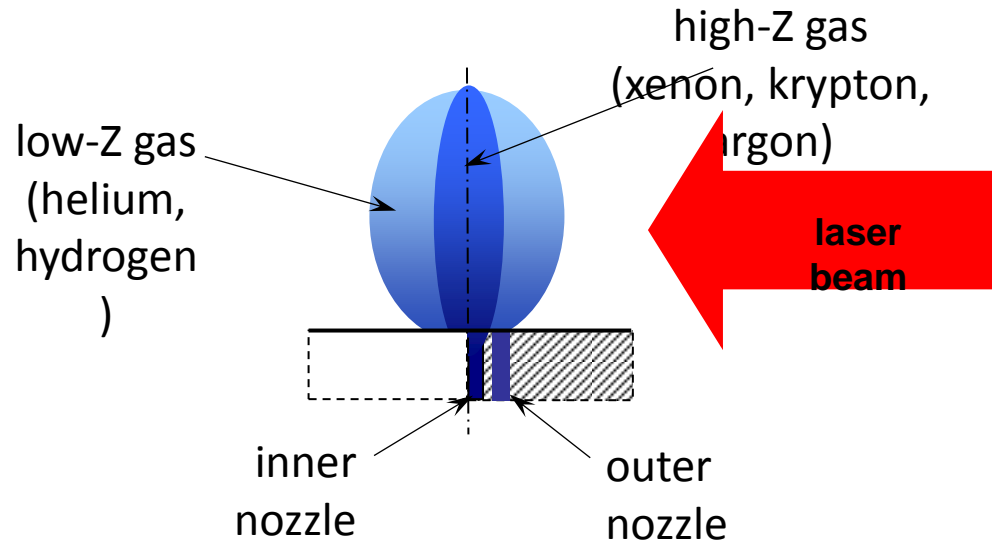
Laser Produced Plasma - solid target



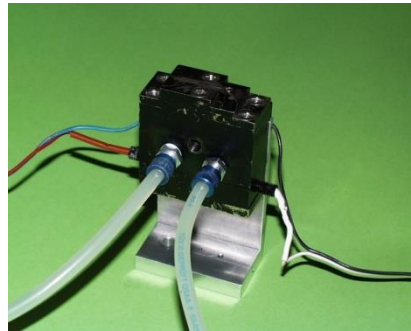
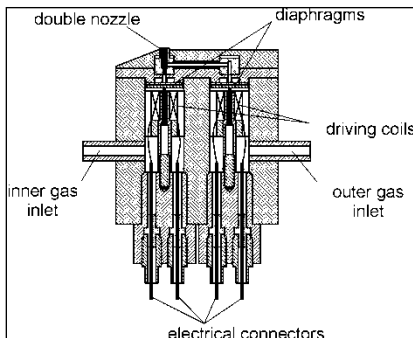
Laser plasma parameters for maximum EUV emission

$\sim 40 \text{ eV}, \sim 10^{19} \text{ cm}^{-3}$

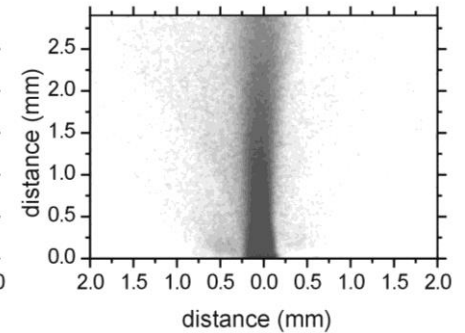
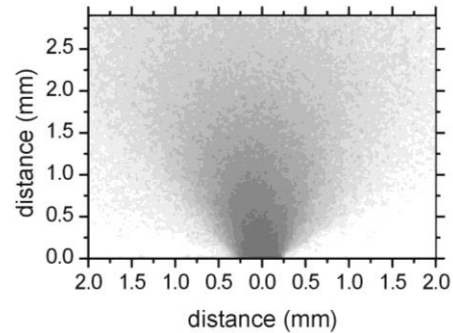
Laser Produced Plasma – gas puff target



- electromagnetic valve system

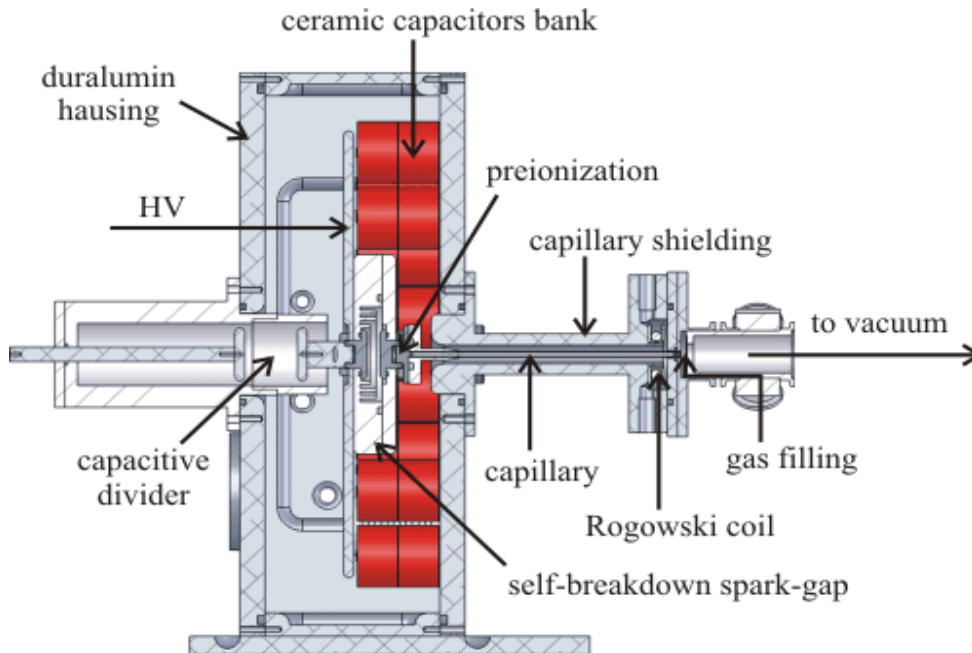


- X-ray backlighting images

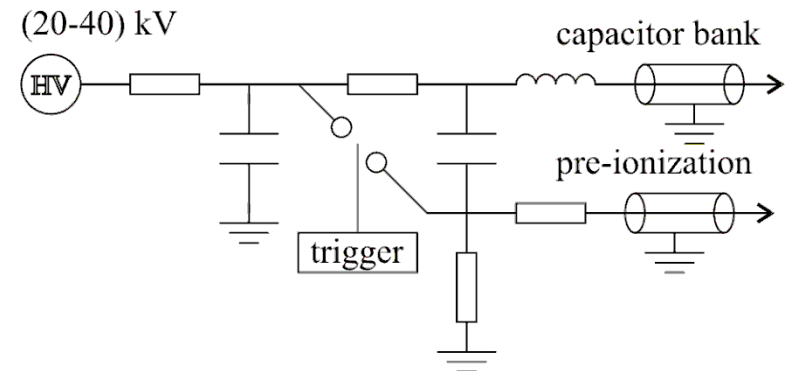


H. Fiedorowicz *et al.* *Appl.Phys. B* 70 (2000) 305; Patent No.: US 6,469,310 B1

Capillary Discharge Plasma

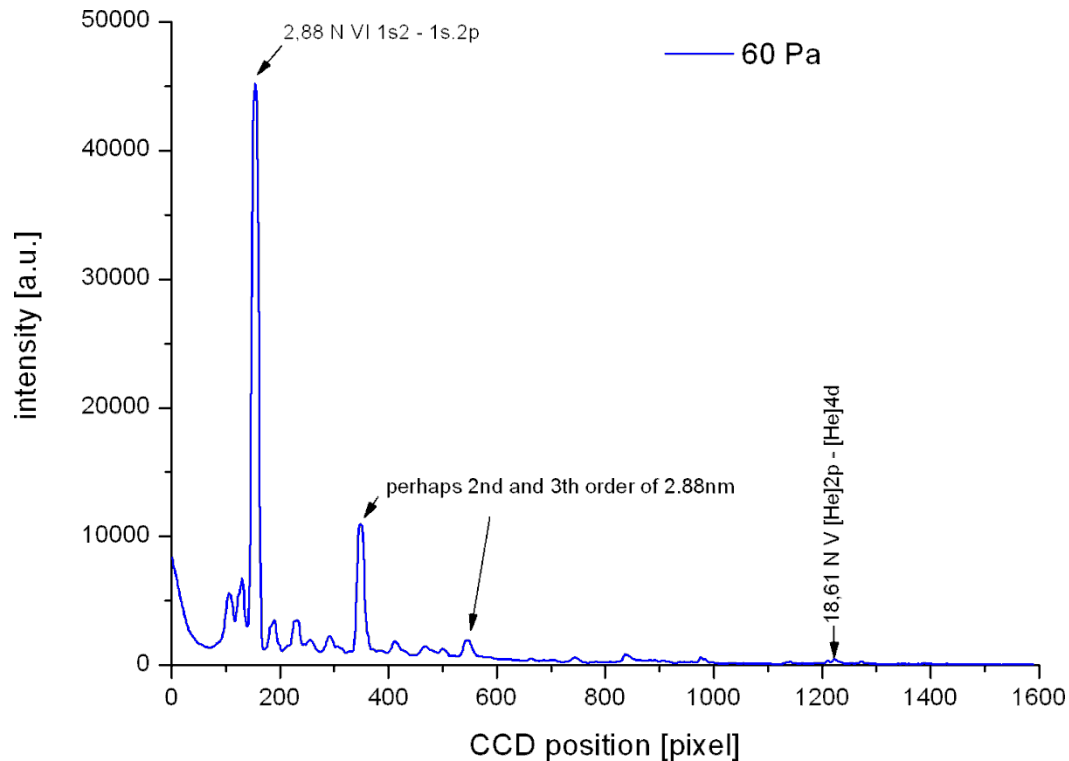


Main discharge unit



- **Ceramic Capacitors (1.25 ÷ 31 nF).**
- **Al₂O₃ capillary, 3.2mm dia., 20cm long.**
- **Low inductance -> high dI/dt.**
- **Pulse-charged: 1x Marx + coil.**
- **Rogowski coil.**

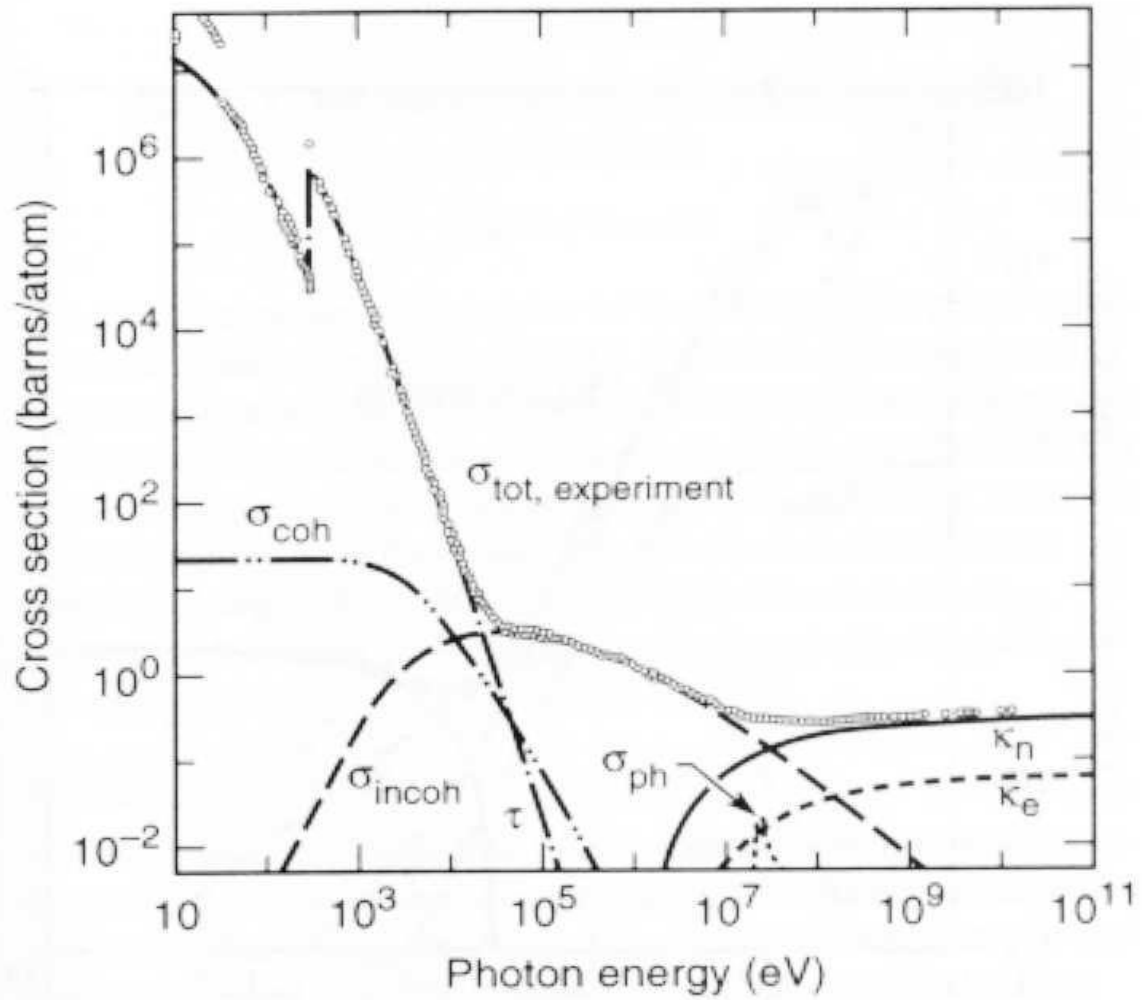
Capillary Discharge Plasma



**Nitrogen spectra 1 ÷ 25 nm
(water window radiation source 200 eV – 500 eV)**

CTU Prague, Fac. Of Nucl. Sci

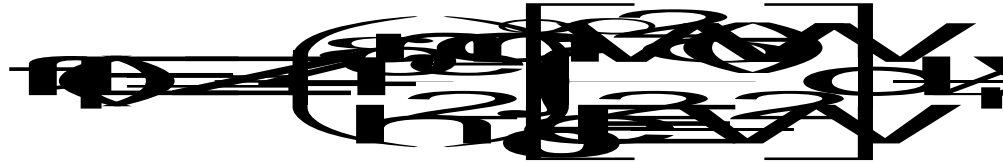
Interaction of X-ray Radiation with Matter



The scattered amplitude:



The factors f_1 and f_2 :



The atomic photoionization cross section:

$$\sigma(\omega) = \frac{A_1}{N_0}$$

The macroscopic factors n and β :

$$n = \frac{e^2 \hbar^2}{2m_e} \bar{f}_1$$

$$\beta = \frac{e^2 \hbar^2}{2m_e} \bar{f}_2$$

The average atomic scattering factors:

$$\bar{f}_1 = \sum_j N_j f_{1j}$$

$$\bar{f}_2 = \sum_j N_j f_{2j}$$

where N_j is the number of atoms of type j per unit volume.

And consequently, using the relation $E = \frac{hc}{\lambda}$:

$$\sigma = \frac{N \left(\frac{h^2}{2mE} \right)^2}{2mE} = \frac{N h^2}{2mE^2}$$

where N is the total number of electrons of type j per unit volume.

Variation of the absorption coefficient away from an absorption edge:

$$\beta = \frac{h^3}{E^2}$$

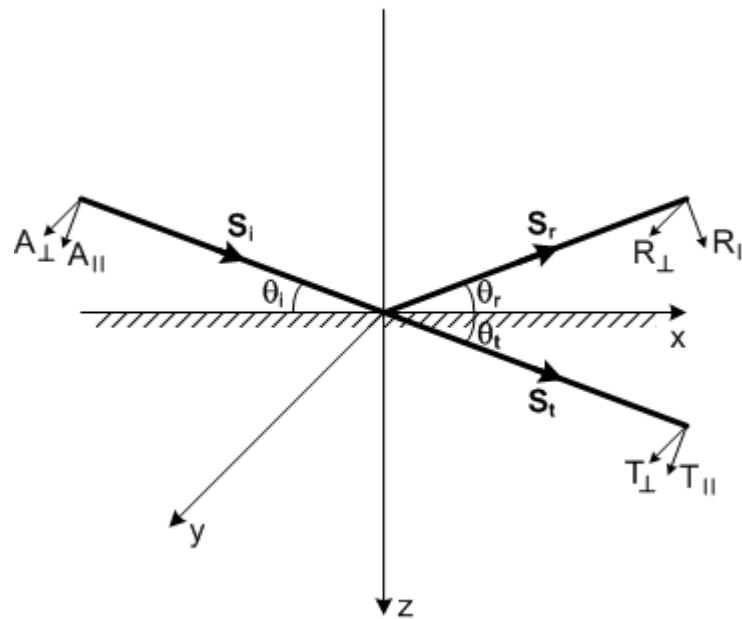
Reflectivity in X-ray region

- Complex index of refraction
- Fresnel equations
- Microroughness

Complex refractive index

$$\tilde{n} = 1 - \delta + i\beta$$

Refraction and Reflection of X-rays



Total external reflection

Fresnel formulas:

$$\begin{aligned} \underline{E}_{\parallel} &= \frac{2n_1 \cos \theta_1}{n_1 \cos \theta_1 + n_2 \cos \theta_2} \underline{E}_{\parallel}^i \\ \underline{E}_{\perp} &= \frac{n_2 \cos \theta_1 + n_1 \cos \theta_2}{n_2 \cos \theta_1 + n_1 \cos \theta_2} \underline{E}_{\perp}^i \end{aligned}$$

$$\begin{aligned} \underline{E}_{\parallel} &= \frac{2n_1 \cos \theta_1}{n_1 \cos \theta_1 + n_2 \cos \theta_2} \underline{E}_{\parallel}^i \\ \underline{E}_{\perp} &= \frac{n_2 \cos \theta_1 + n_1 \cos \theta_2}{n_2 \cos \theta_1 + n_1 \cos \theta_2} \underline{E}_{\perp}^i \end{aligned}$$

$$\begin{aligned} \underline{E}_{\parallel} &= \frac{2n_1 \cos \theta_1}{n_1 \cos \theta_1 + n_2 \cos \theta_2} \underline{E}_{\parallel}^i \\ \underline{E}_{\perp} &= \frac{n_2 \cos \theta_1 + n_1 \cos \theta_2}{n_2 \cos \theta_1 + n_1 \cos \theta_2} \underline{E}_{\perp}^i \end{aligned}$$

$$\begin{aligned} \underline{E}_{\parallel} &= \frac{2n_1 \cos \theta_1}{n_1 \cos \theta_1 + n_2 \cos \theta_2} \underline{E}_{\parallel}^i \\ \underline{E}_{\perp} &= \frac{n_2 \cos \theta_1 + n_1 \cos \theta_2}{n_2 \cos \theta_1 + n_1 \cos \theta_2} \underline{E}_{\perp}^i \end{aligned}$$

Reflectivity R_p and R_s :

$$R_p = \frac{R_{\perp}}{A_{\perp}} \left(\frac{R_{\parallel}}{A_{\parallel}} \right)^*$$

$$R_s = \frac{R_{\parallel}}{A_{\parallel}} \left(\frac{R_{\perp}}{A_{\perp}} \right)^*$$

Surface microroughness is important:

$$R = R_F R_{\sigma}$$

$$R = \exp(-4\pi\sigma\phi/\lambda)$$

X-Ray Optics

Reflective optics

Capillaries, polycapillaries, parabolic, elliptic and foil mirrors, paraboloidal and ellipsoidal mirrors. K-B system, Wolter system

No monochromatisation, but hard energy cut-off

Refractive optics

Multiple Lenses

Microfabricated Kinoform structures

Diffractive optics

Crystals

Multilayered structures

Fresnel lenses

X-RAY OPTICS BASED ON REFRACTION

X-RAY LENS

REFRACTIVE INDEX

$$n=1-\delta-i\beta \quad (1)$$

$$\delta=0.5 (E_p/E)^2 \sim 10^{-4}-10^{-7}, \quad \beta=1/4\pi \mu\lambda \sim 10^{-3}-10^{-5}$$

E_p — plasmon energy, E — photon energy, λ — wavelength, μ — absorption

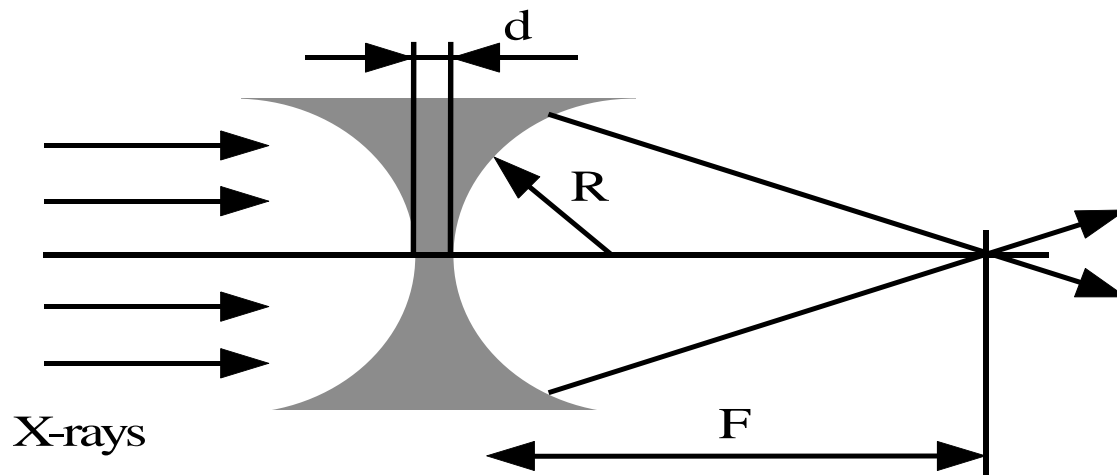


Fig.1

R — curvature radius, d — lens thickness.

Lens focal length

$$F=R / 2\delta \quad (2)$$

COMPOUND X-RAY LENS

Compound lens focal length : $F = R / 2\delta N$ (1),

N– number of individual lenses

A.Snigirev, V.Kohn, I.Snigireva, B.Lengeler, “A Compound Refractive lens for focusing high-energy X-rays”, Nature (London) **384**, 49 (1996).

15 keV X-rays

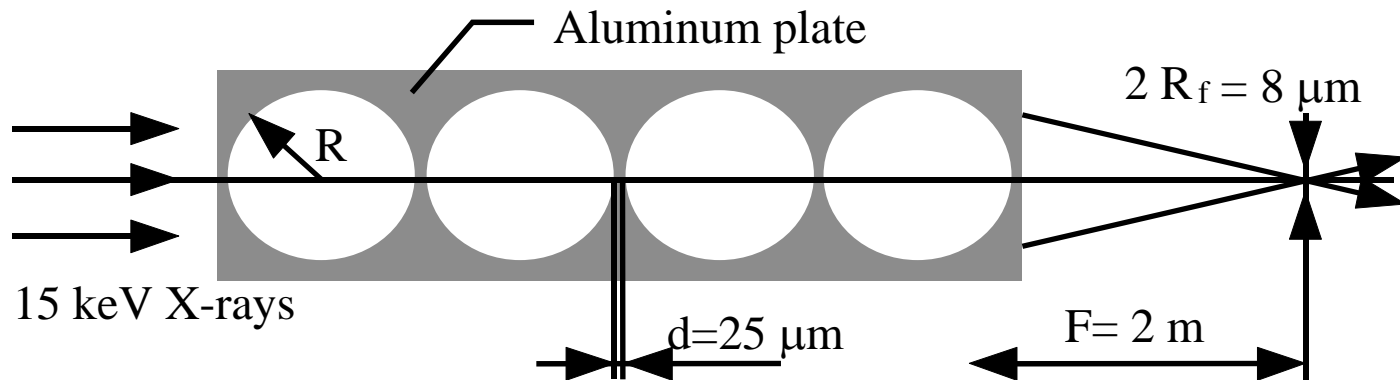
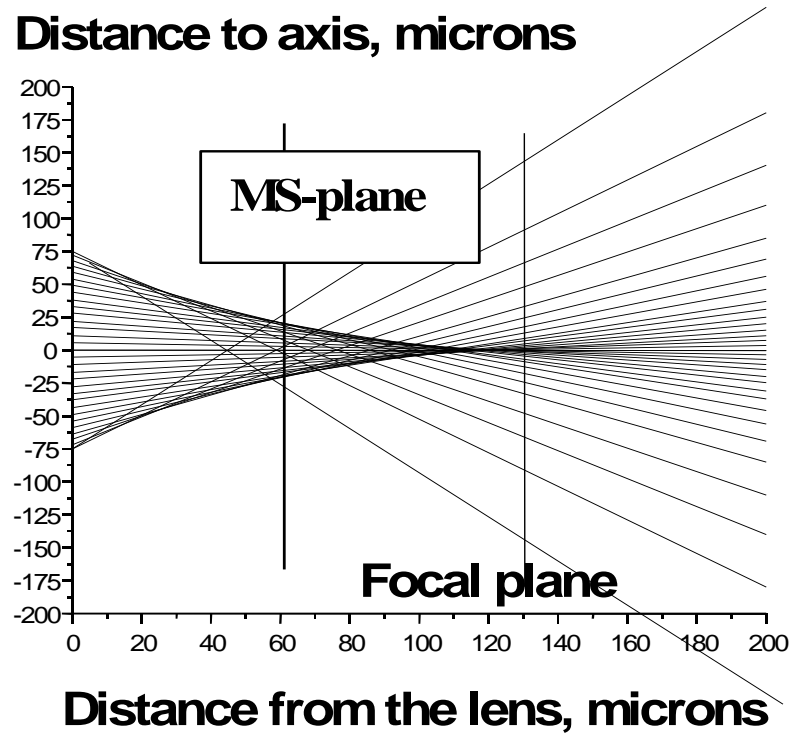


Fig. 1

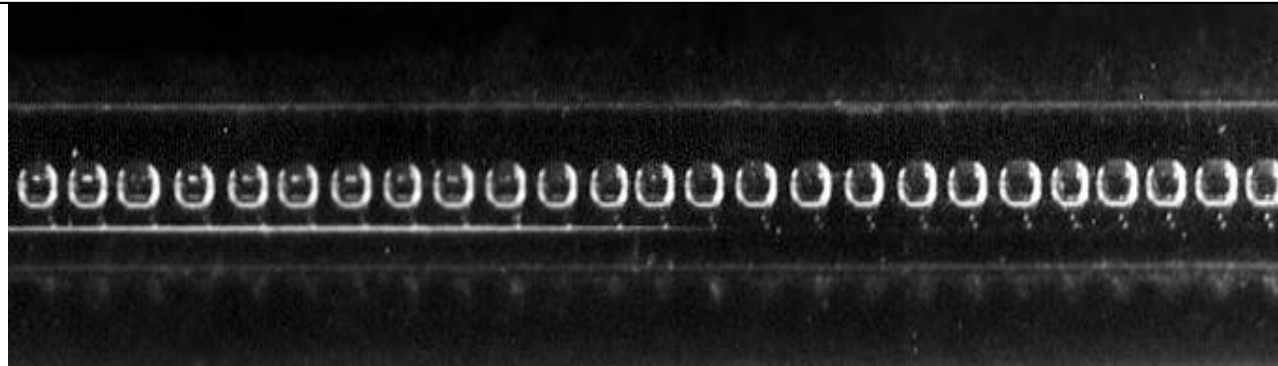
$R = 0.3 \text{ mm}$, $N = 30$, intensity gain $G = 3$

SPHERICAL ABERRATIONS AND SPOT SIZE OF THE MICROCAPILLARY OR BUBBLE LENS

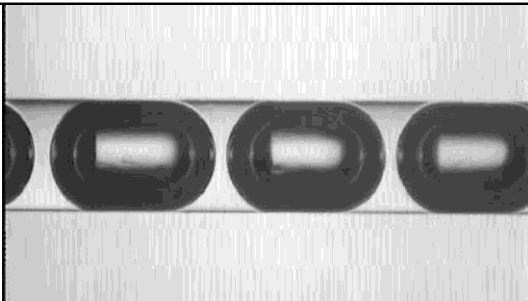


**Fig 1. Paths of 8 keV X- rays forming a focal spot of the X- ray lens.
Individual lens radius is 100 microns.
The number of microlenses is $N = 103$.**

Photographs of epoxy microcapillary compound refractive lens



Capillary diameter = **0.8 mm**



Capillary diameter = **0.2 mm**

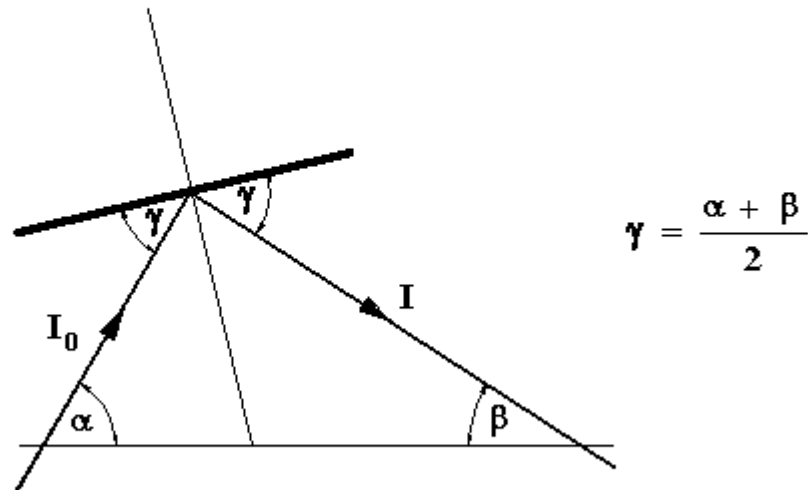
GRAZING INCIDENCE X-RAY MIRRORS

Grazing Incidence Optics

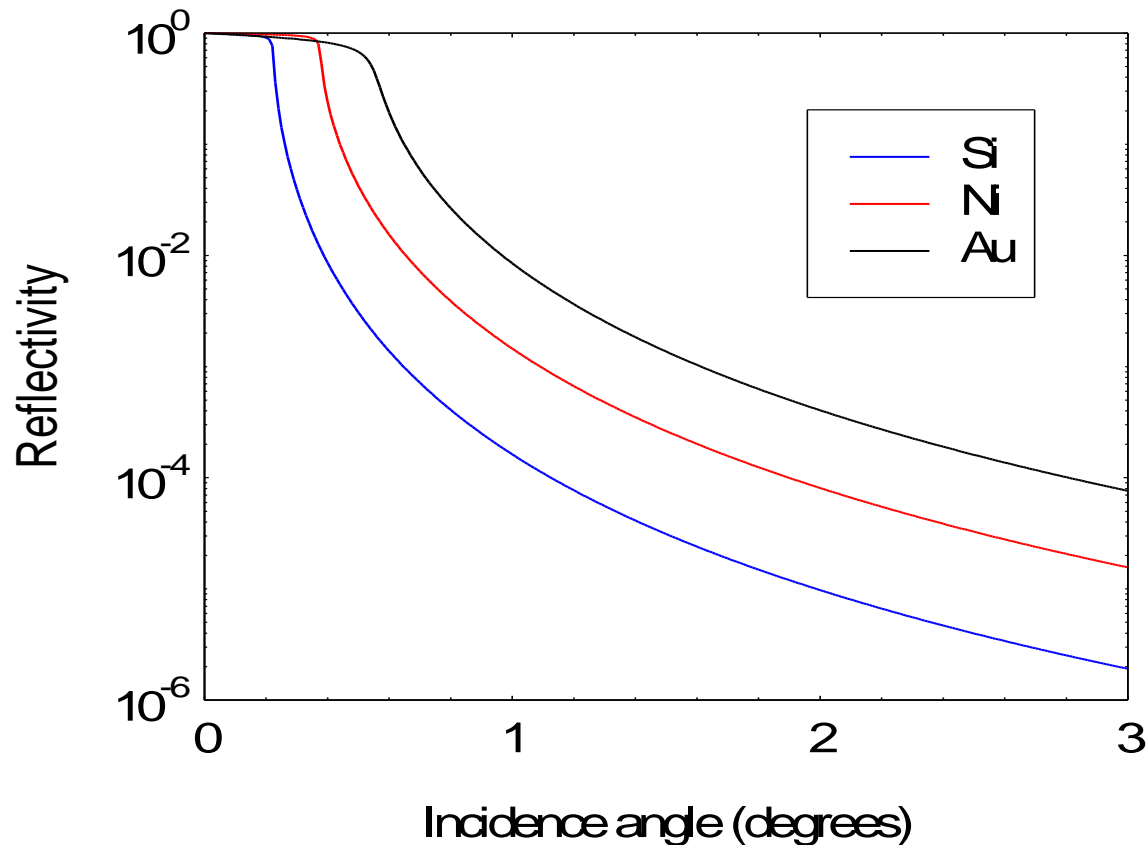
- Total external reflection
 - Capillaries, polycapillaries
 - Parabolic, elliptic and foil mirrors, paraboloidal and ellipsoidal mirrors
 - Kirkpatrick-Baez optic
 - Wolter optic
 - No monochromatisation, but hard energy cut-off

Flat X-ray Mirror

FLAT MIRROR



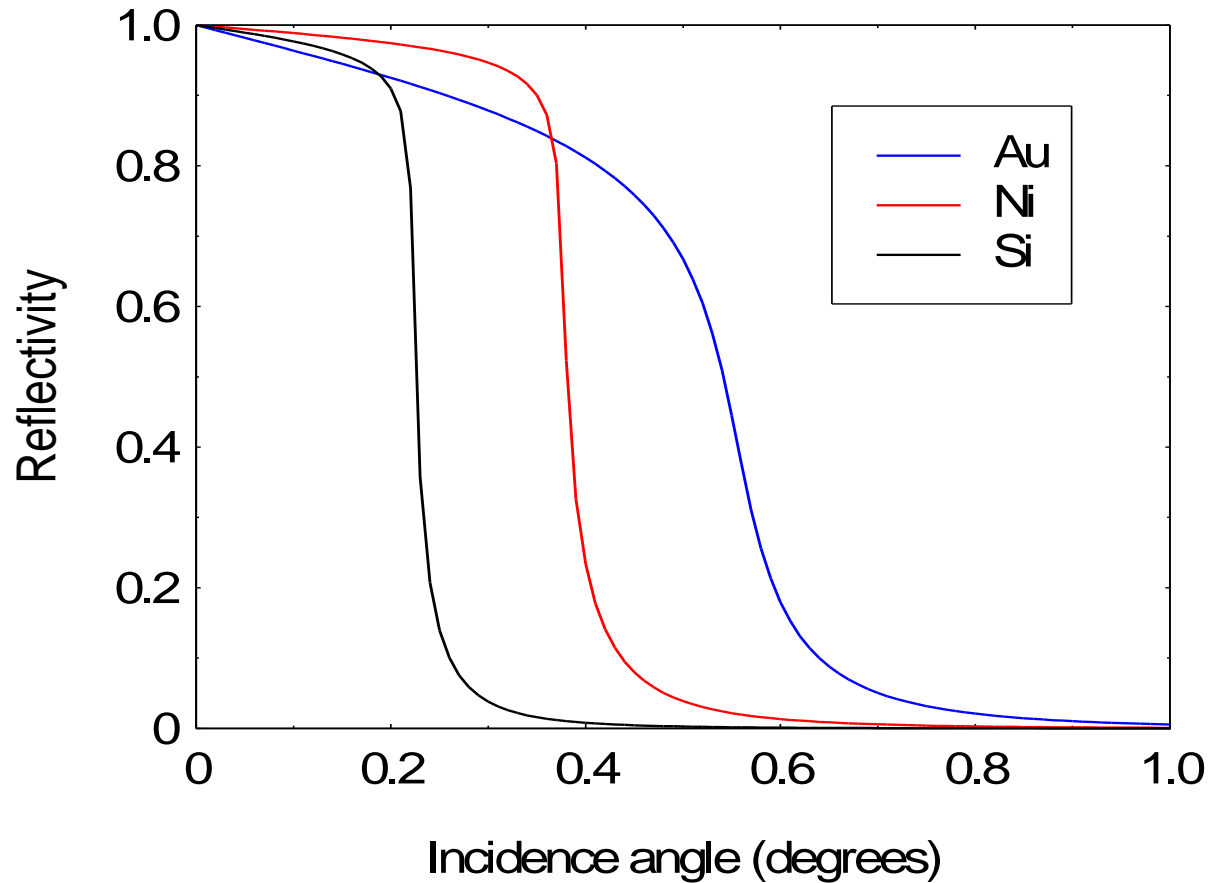
Grazing Incidence Reflectivity



Refractive index $n < 1$, total external reflection.
Critical angle rises with atomic number as $Z^{1/2}$.
Beyond critical angle intensity falls as θ^{-4} or faster

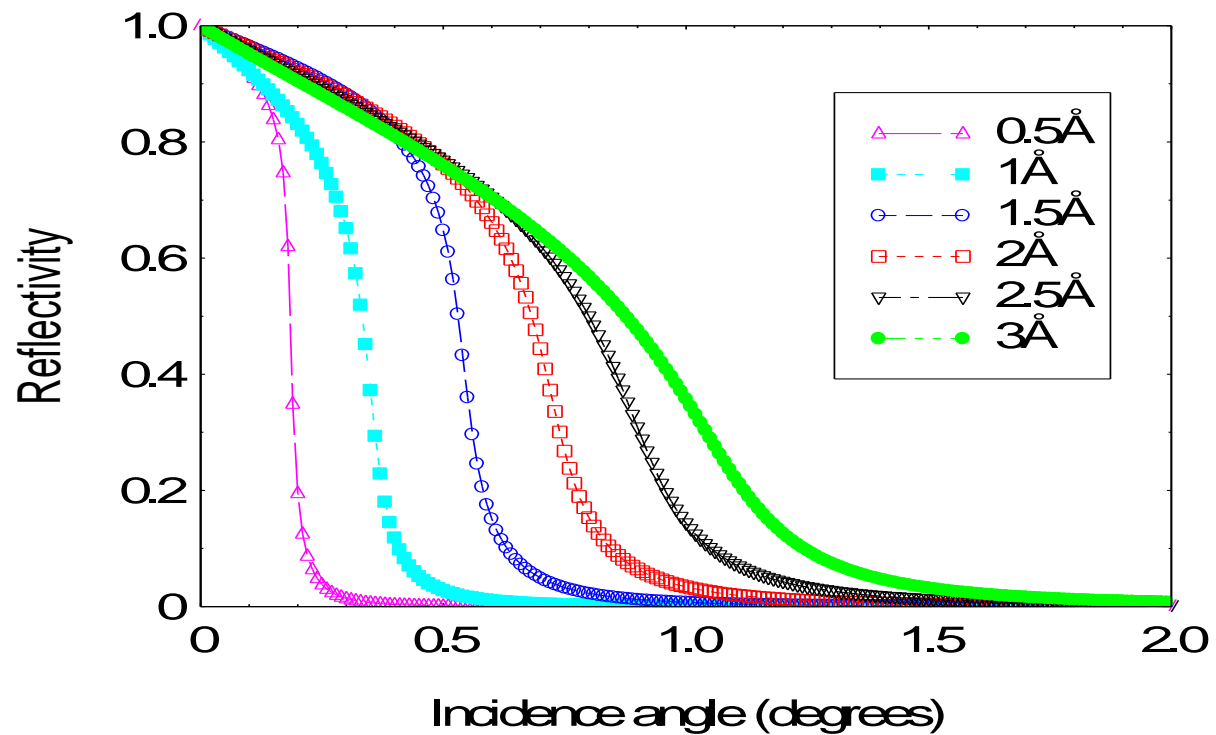
Grazing-incidence reflectivity for Au, Ni and Si

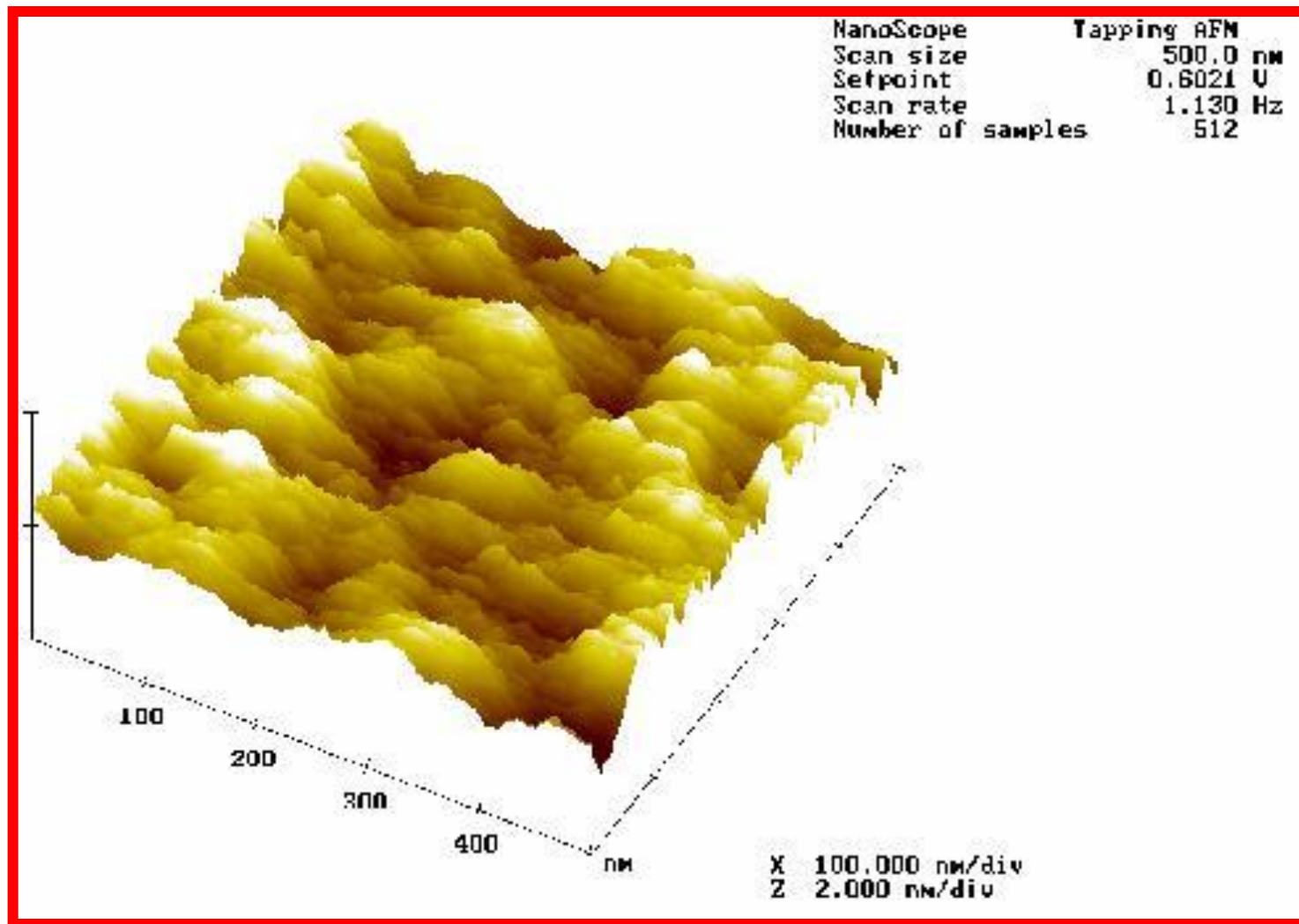
1.54Å wavelength



Absorption reduces reflectivity near the critical angle

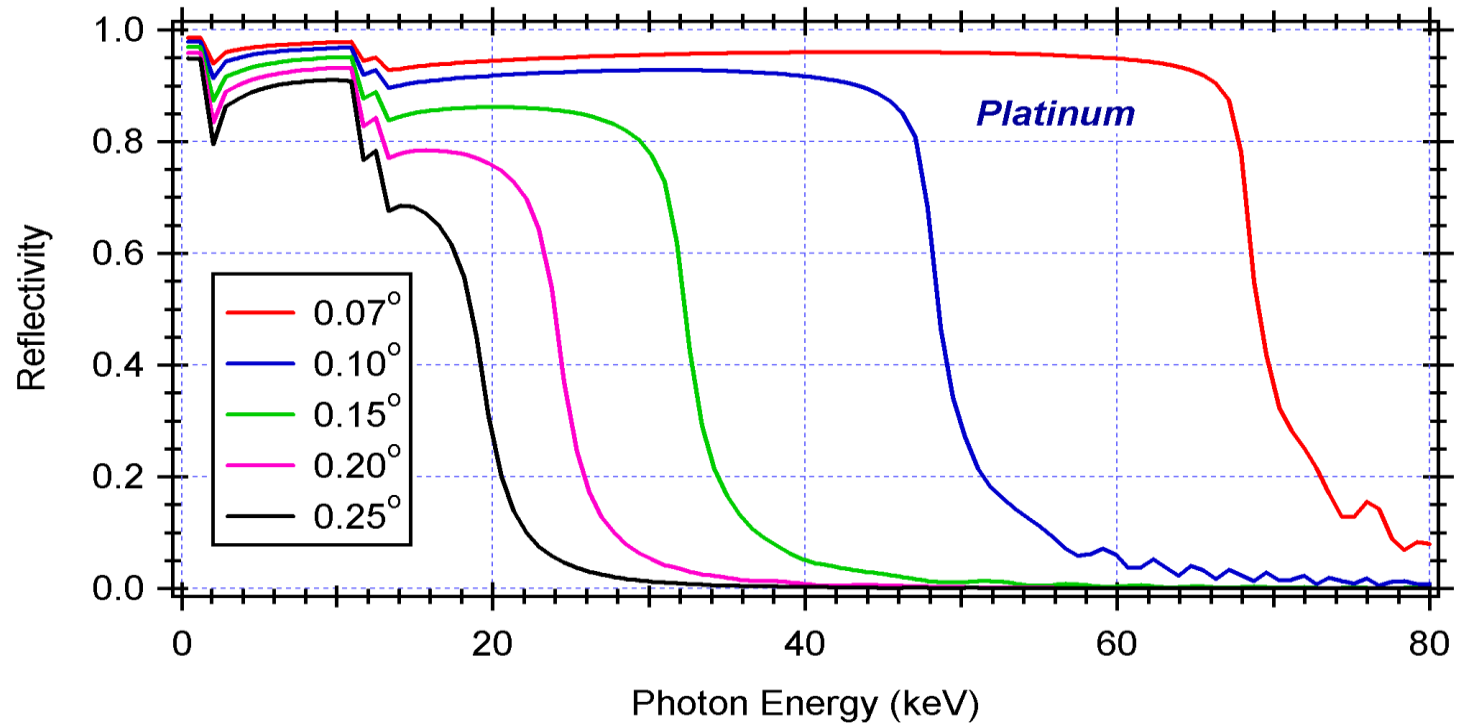
Variation of reflectivity with X-ray wavelength (Au)



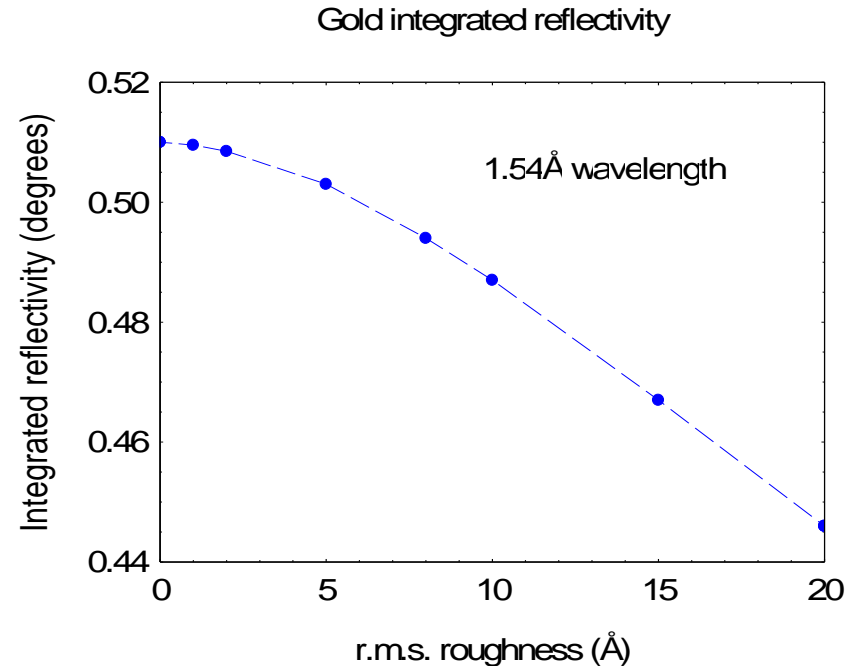
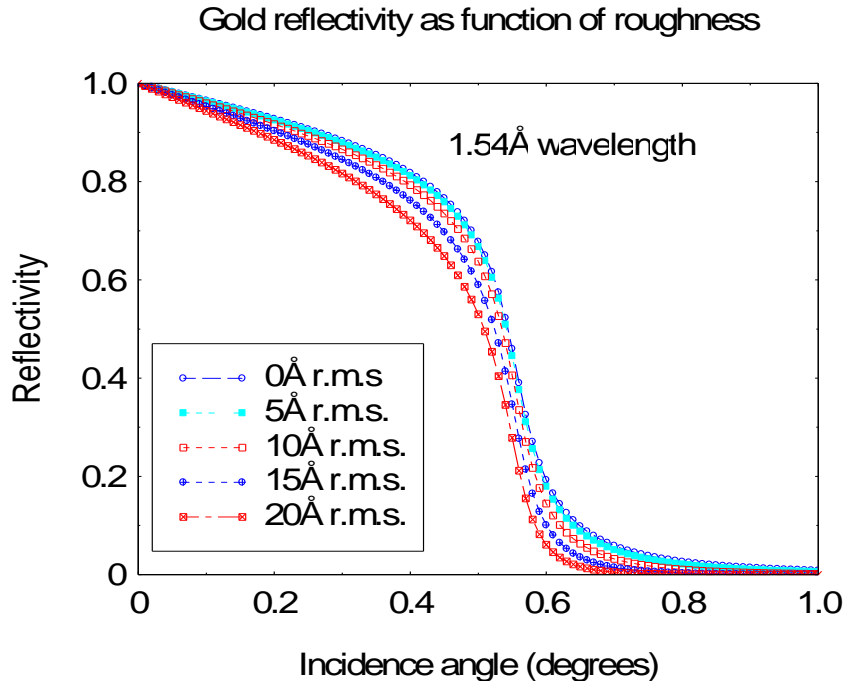


**Tapping AFM images of the surface of the double - sided flats developed for Schmidt lobster-eye telescopes. The resulting microroughness RMS is 0.3 nm.
Test facility at the Astronomical Observatory in Brera, Italy.**

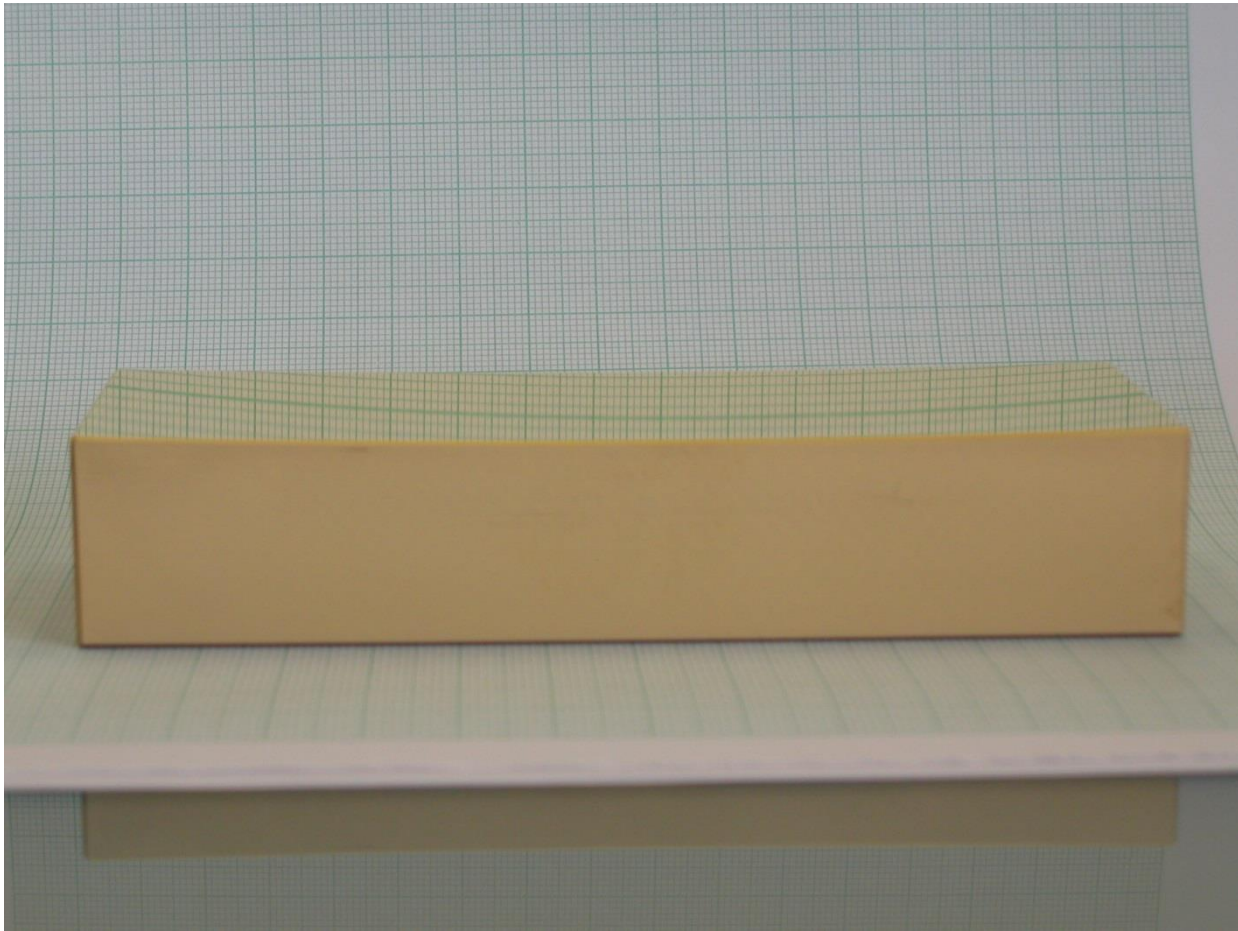
Effect of Grazing Angle



Effect of Surface Microroughness

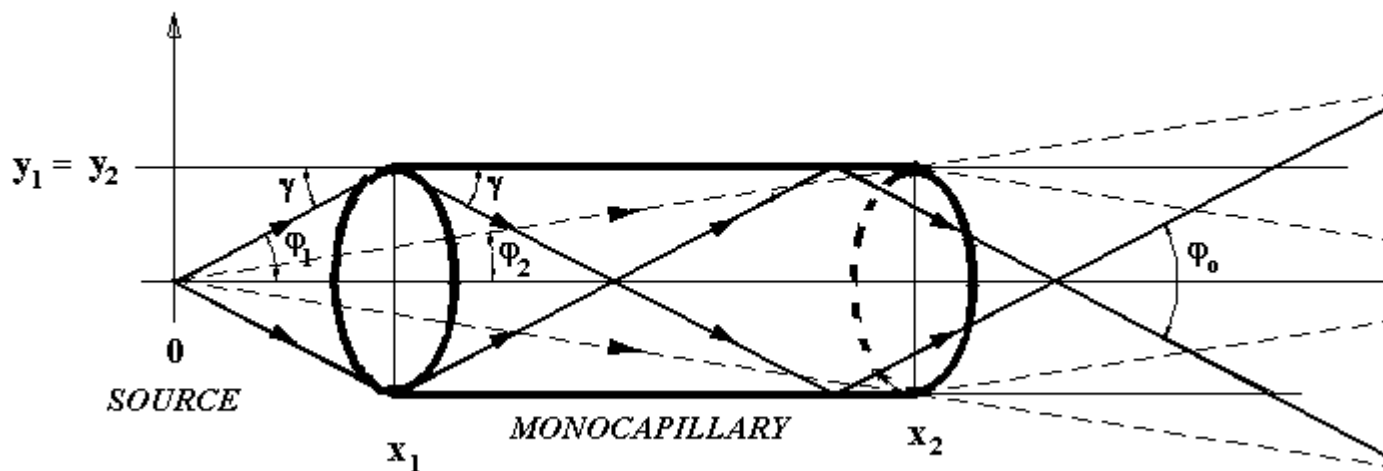


Unlike the reflectivity beyond the critical angle, the effect of roughness is relatively small.
Loss of only 5% for roughness of 1nm (10Å)

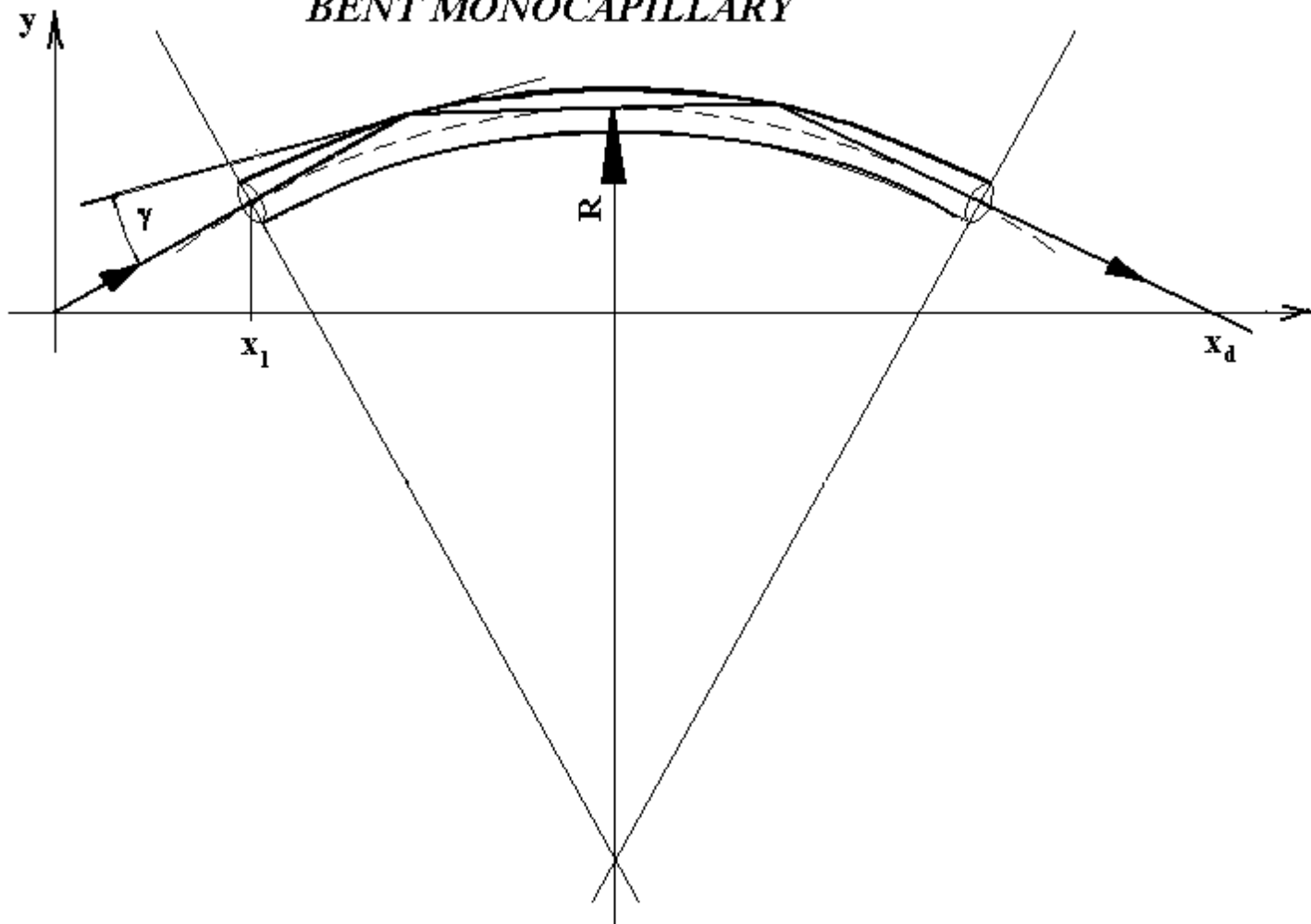


Monocapillary (SC) geometry and description

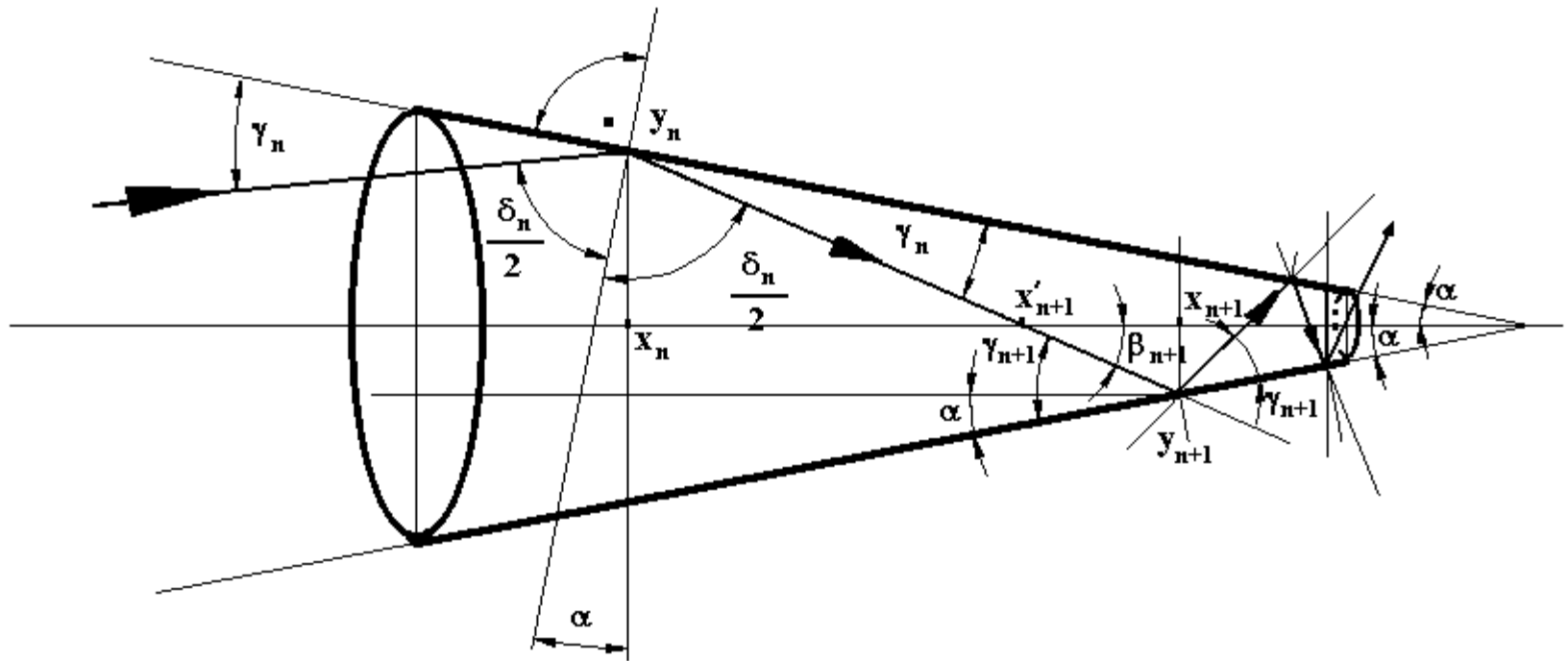
SINGLE CAPILLARY (MONOCAPILLARY)



BENT MONOCAPILLARY

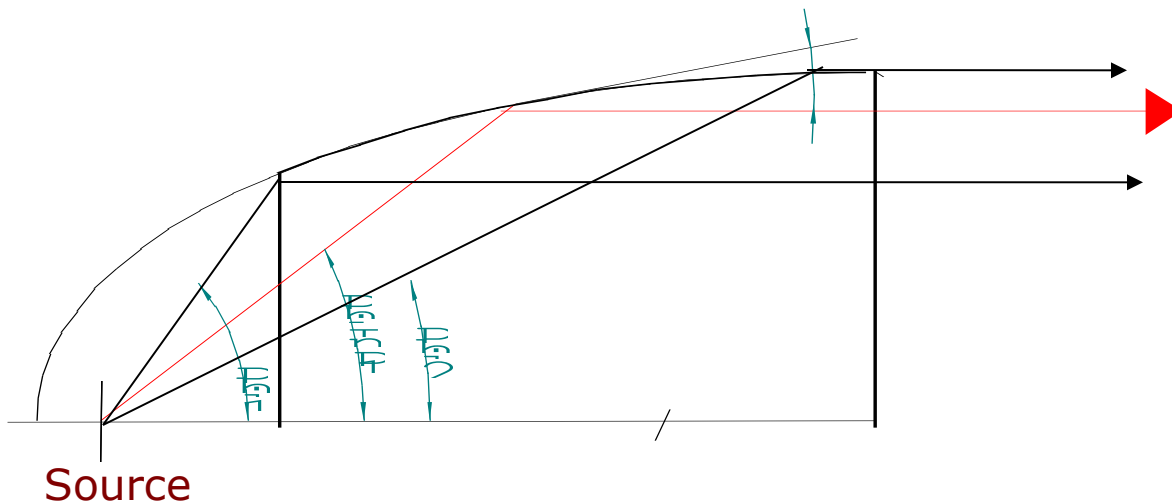


TAPERED MONOCAPILLARY

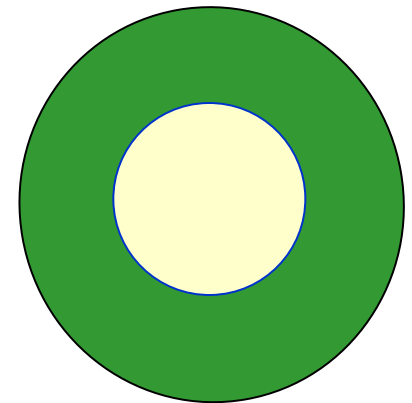


Paraboloidal Mirror

Highly parallel beam (< 1 mr)
Large area - circa 1 mm diameter
Hole in the middle



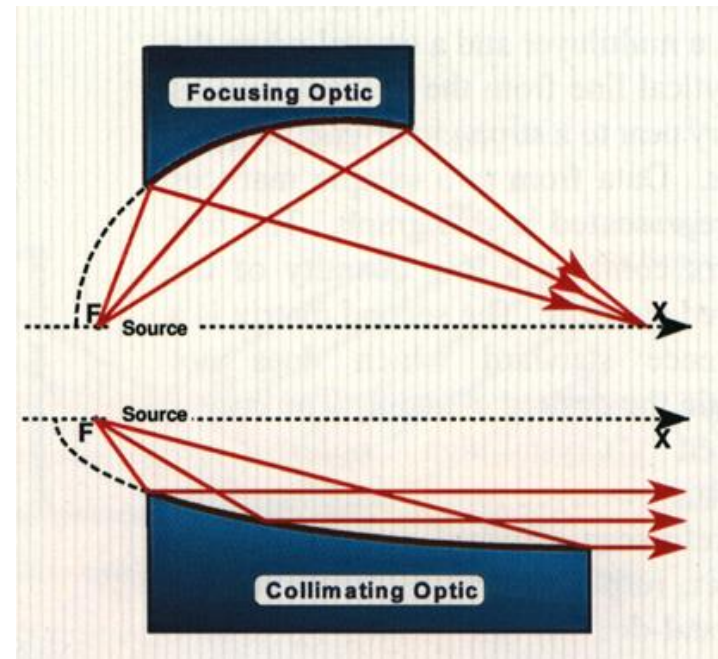
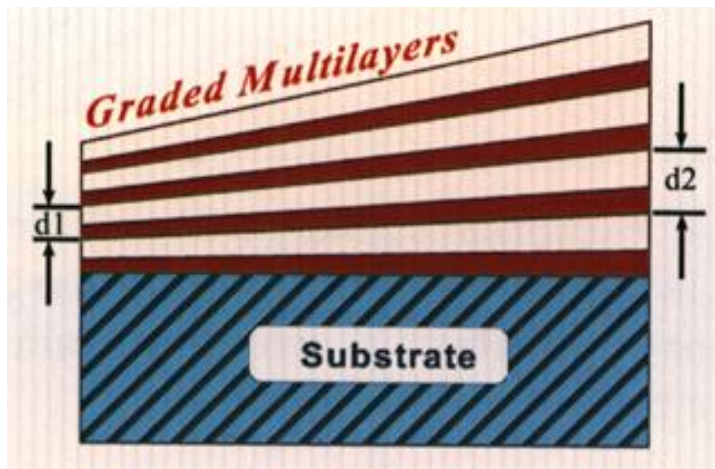
Beam profile



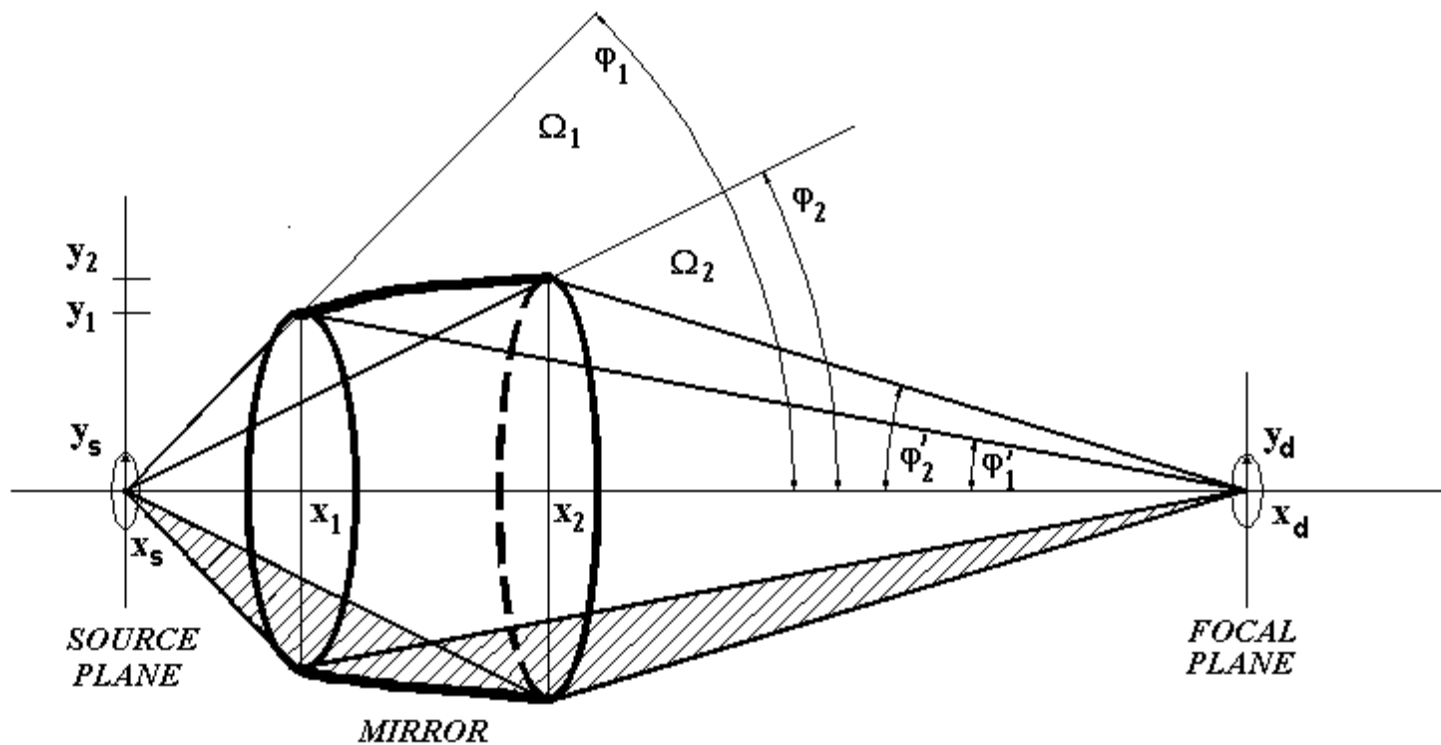
Optimum efficiency in coupling to monochromator
Precise alignment necessary

X-ray Optics

Multilayer Mirrors



ELLIPSOIDAL MIRROR

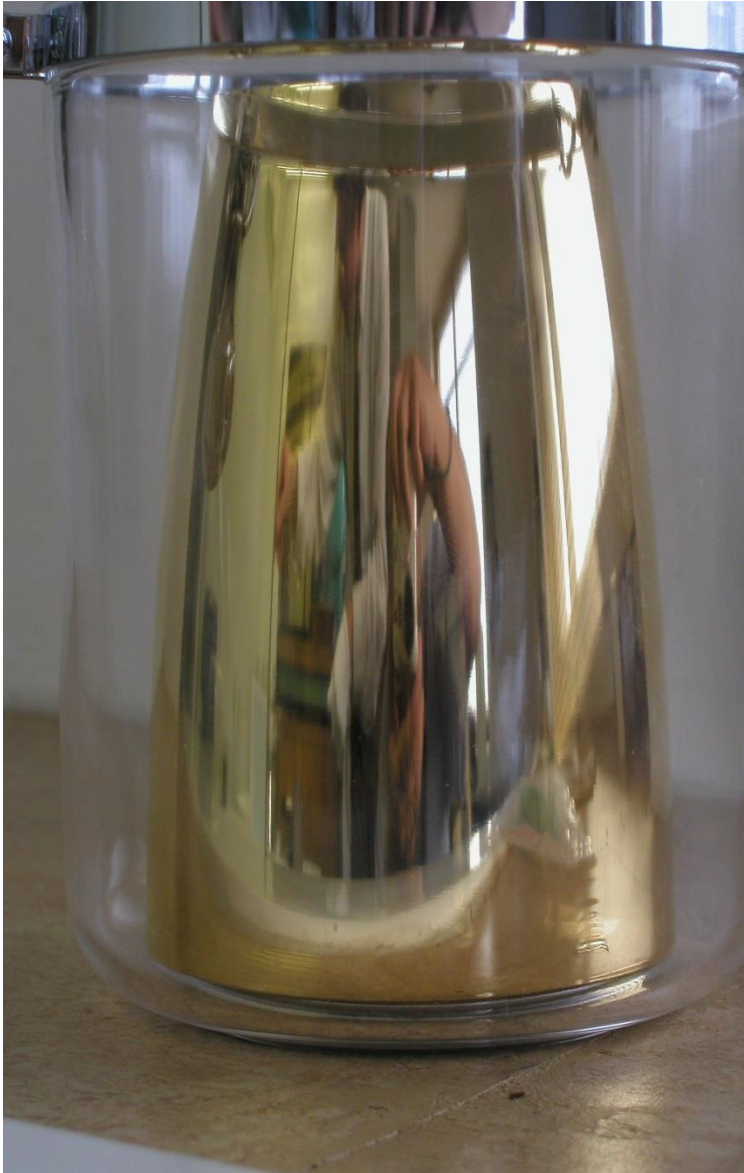


Replicated X-ray Optics –



Replicated Wolter 1 X-ray mirrors of the KORONAS satellite (aperture 80 mm)

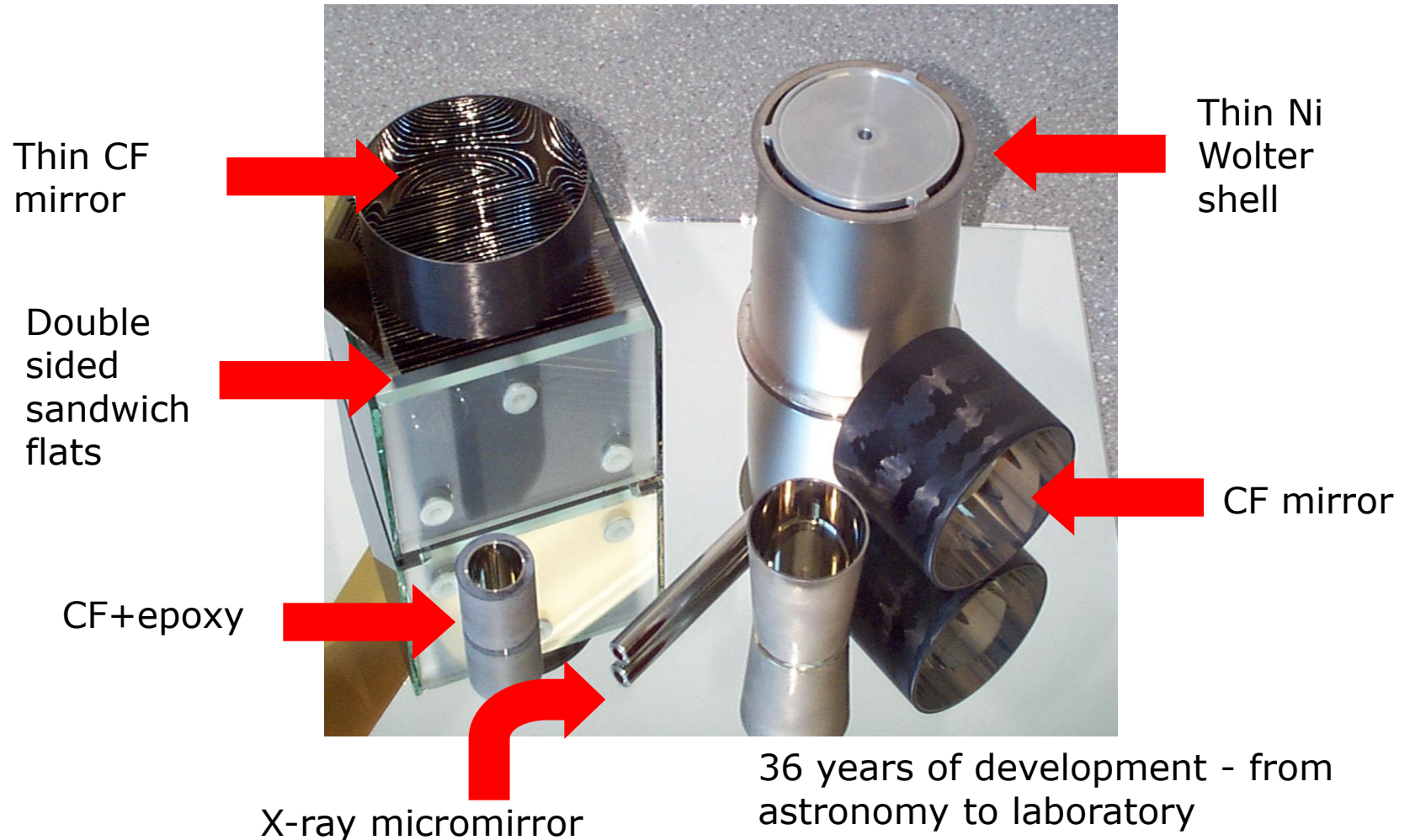
EXTATIC Prague, September 2017



MANDREL

Grazing Incidence X-Ray Optics

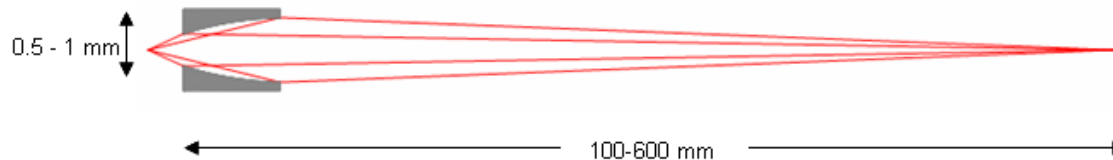
Samples of replicated grazing incidence X-ray optics



Ellipsoidal X-ray Mirror

Ellipsoidal Micromirror™

- Apertures as small as 0.4 mm dia
- Mirrors optimised for 8 keV
- Grazing angle 9.5 mrad at the mirror input
(Au coated reflecting surface)
- Au or Ni surface
- Convergence / Divergence lower than 1.5 mrad (ellipsoidal mirrors)
- Convergence / Divergence lower than 0.1 mrad (parabolic mirrors)

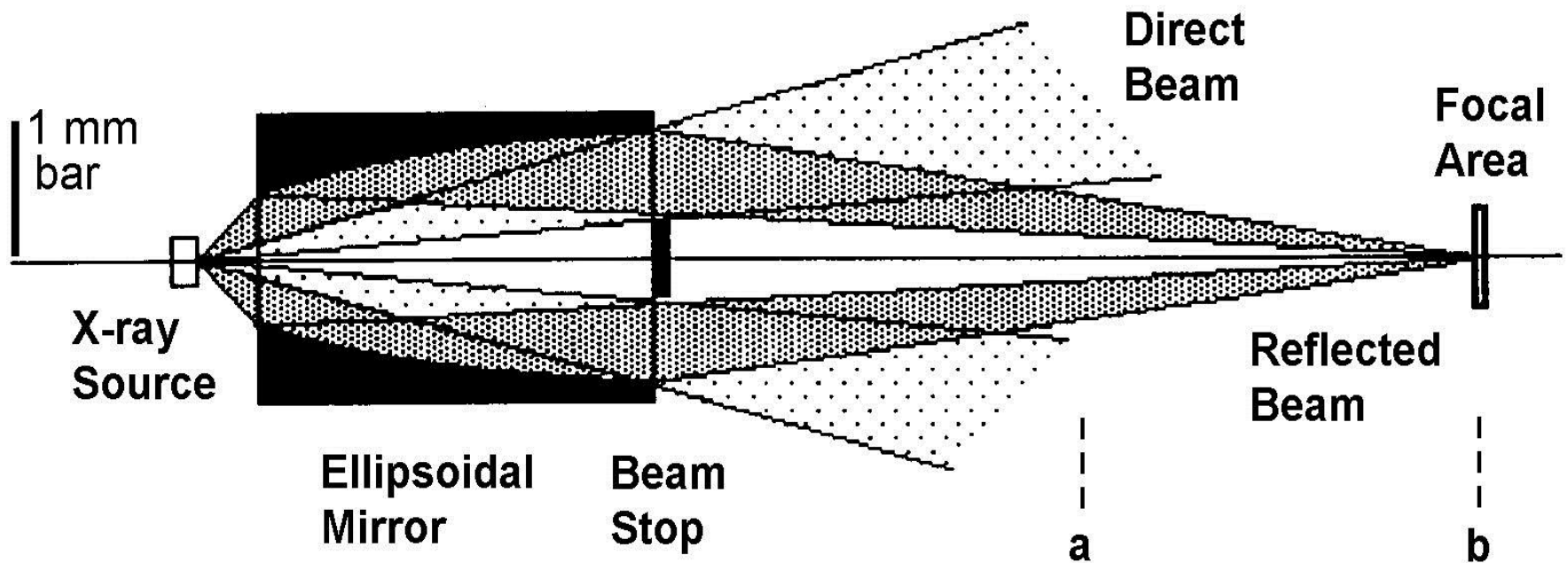


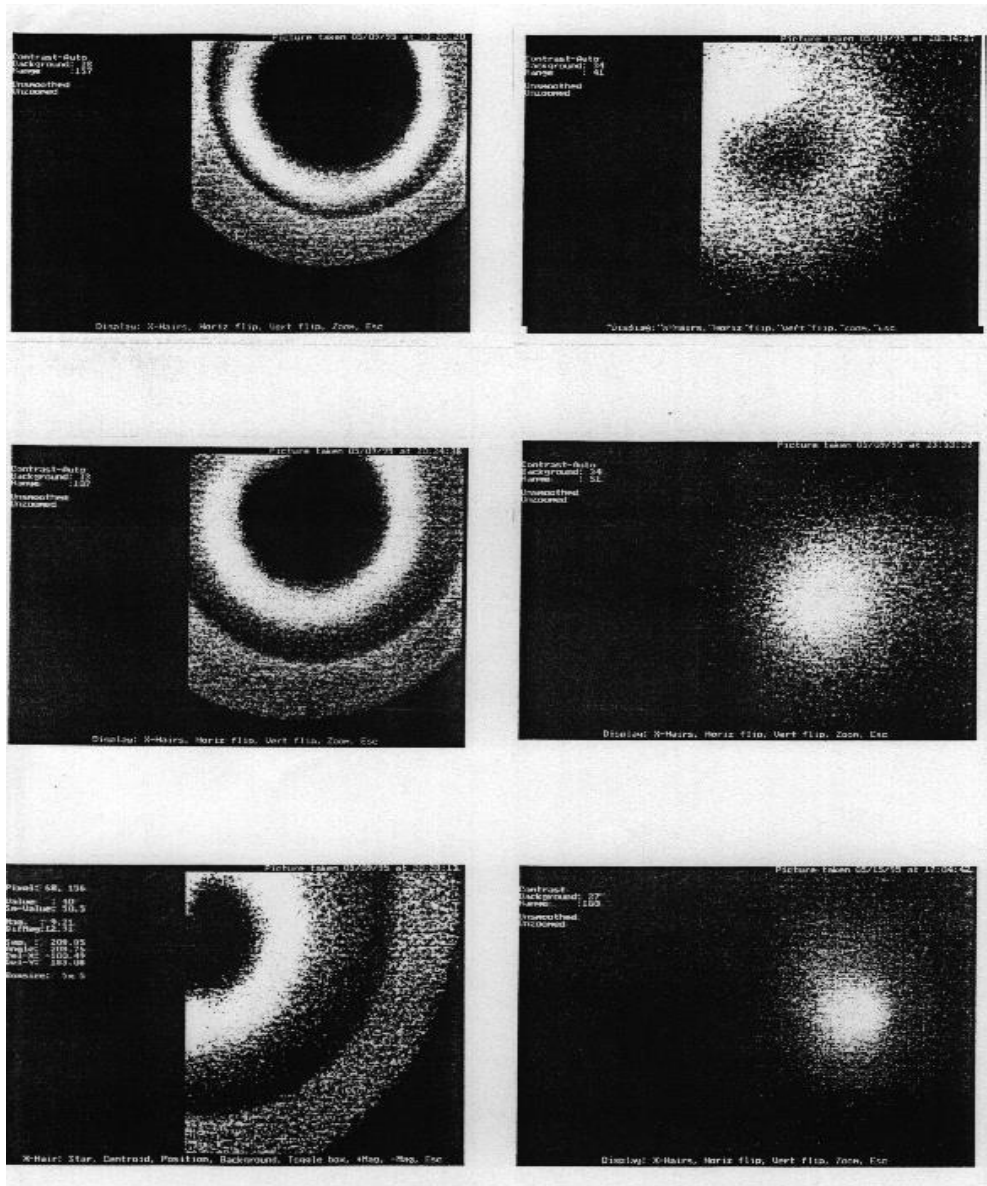
Vacuum Test Bench for X-ray Cameras and Optics



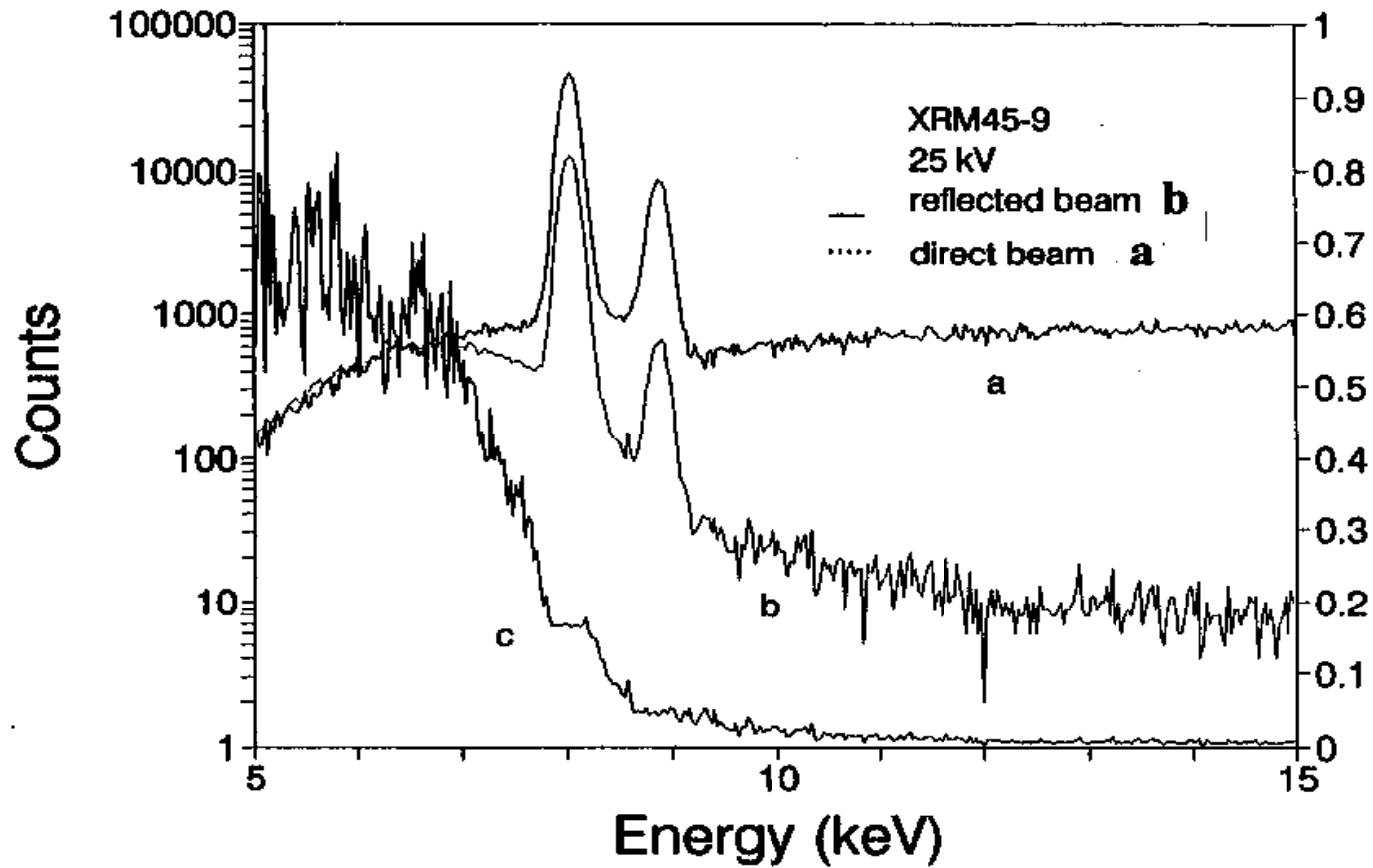
0 mm Y-AXIS IN THE SAME SCALE AS X-AXIS 400 mm

Y-AXIS NOT IN THE SAME SCALE AS X-AXIS

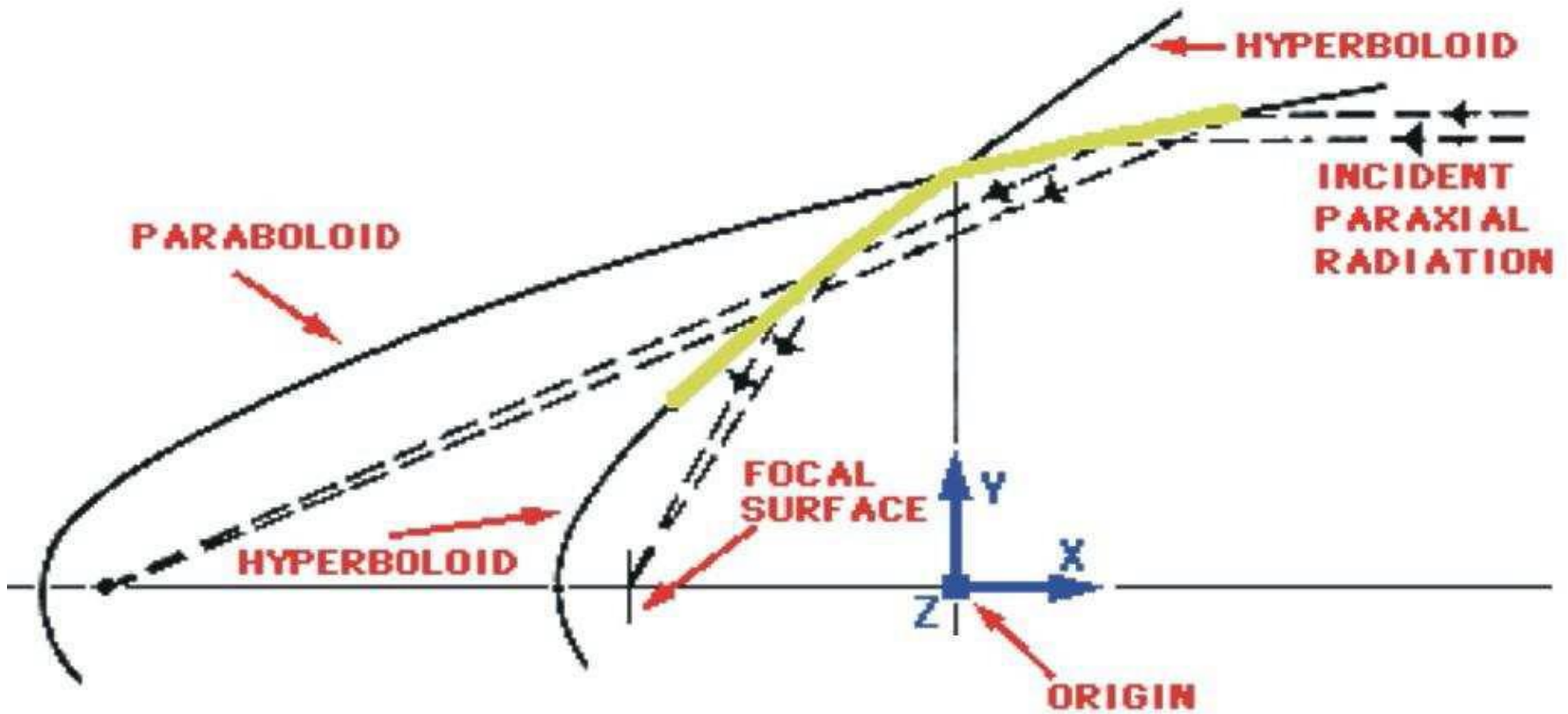




Ellipsoidal X-ray Mirror as a Spectral Filter



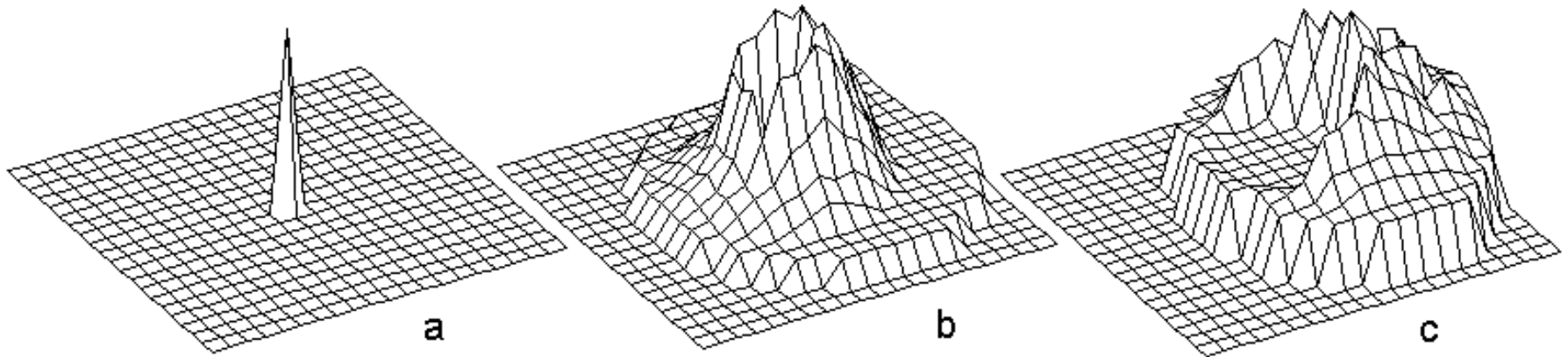
Wolter Optic



Computer simulations

(virtual CCD images)

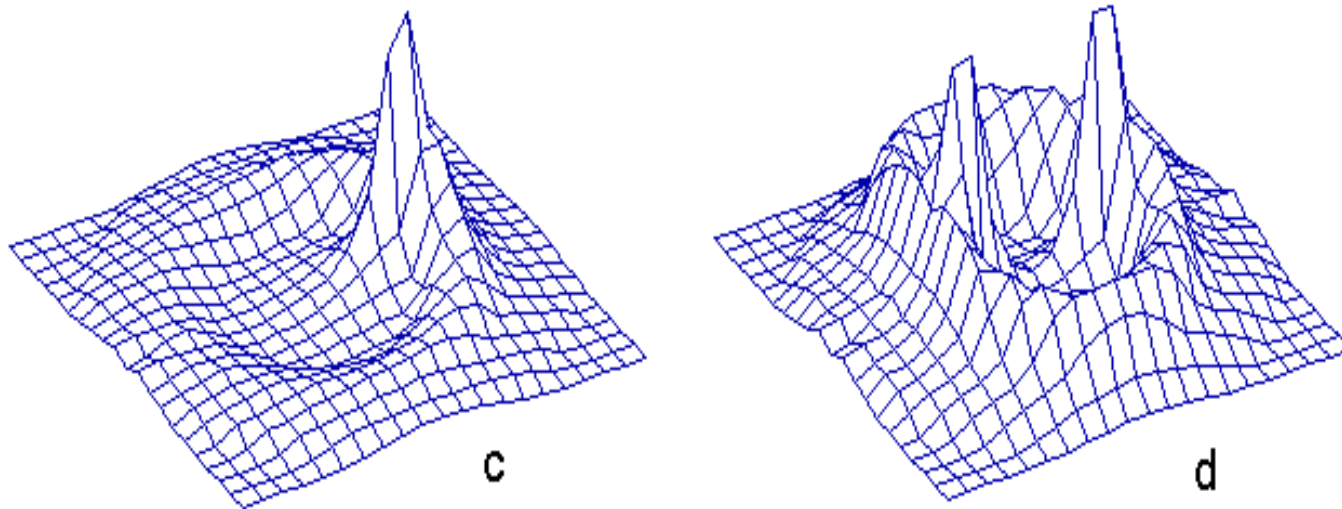
Focal spots for off-axis source position



Graphs **a** to **c** show the effect of point-like X-ray source off-axis displacement on the detector intensity distribution for ellipsoidal mirror.

- a** – 0 μm source displacement,
- b** – 200 μm displacement,
- c** – 400 μm displacement.

Focal spots for off-axis source position



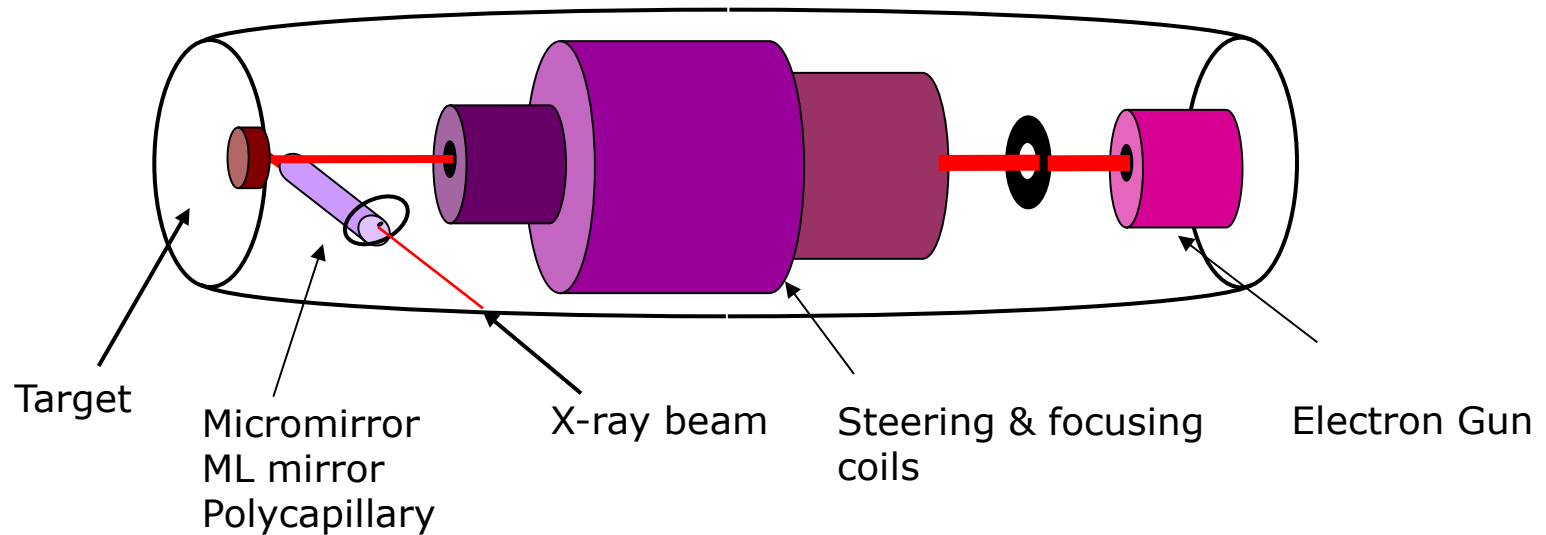
Detector intensity distribution for line X-ray source for ellipsoidal mirror.

c – asymmetric line X-ray source 0 - 100 μm from the axis,

d – symmetric line X-ray source 0 to +50 μm and 0 to +50 μm around the axis.

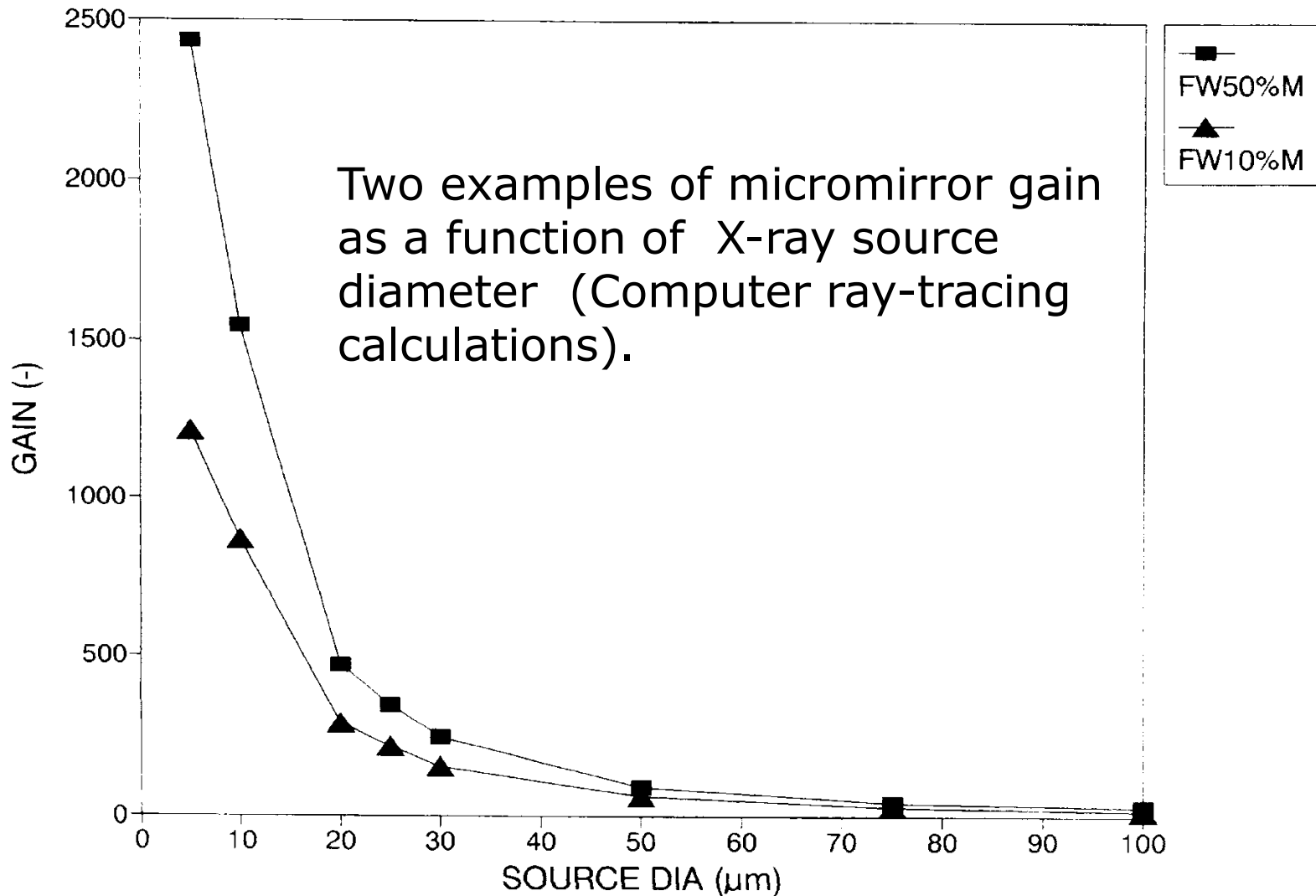
MicroSOURCE®

X-ray source – X-ray mirror combination

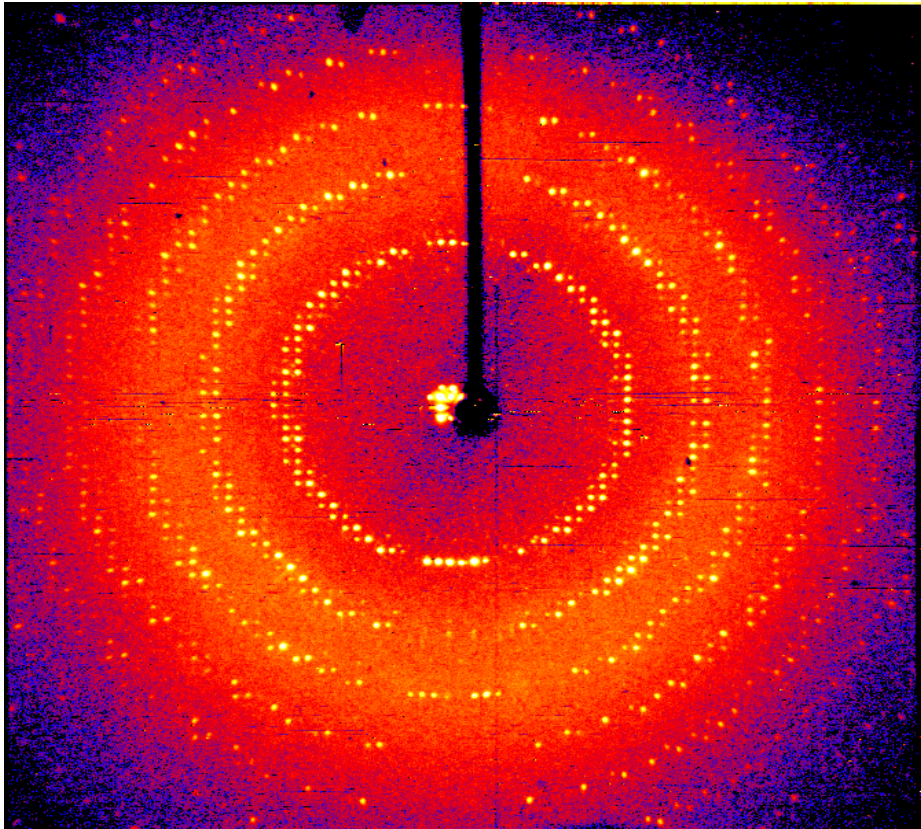


- The focus may be changed from spot to line electronically
- Stability of focal spot assured
- Modular design allows ease of access for tube changes
- Patents
- Focal spot size, shape and position are controlled automatically

Source – X-ray Optic combination (The importance of source size)



Nonius KappaCCD₂₀₀₀



Courtesy of Nonius B.V.

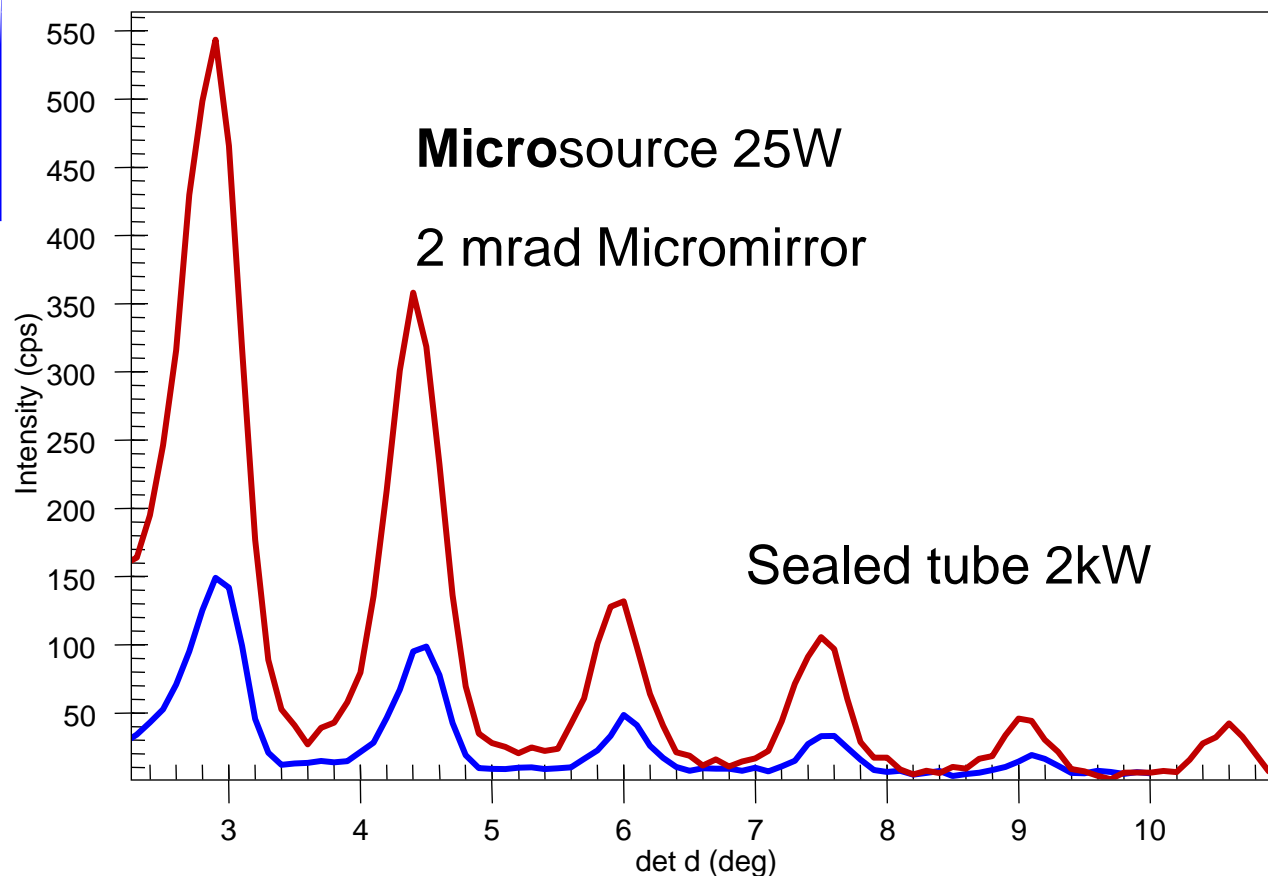
Lysozyme single crystal

Unit cell aligned to the direction of the X-ray beam using 180 secs per 2° rotation

Excellent performance in terms of brightness, low background noise, small beam size. and ease of use

Powder Diffraction

Silver Behenate



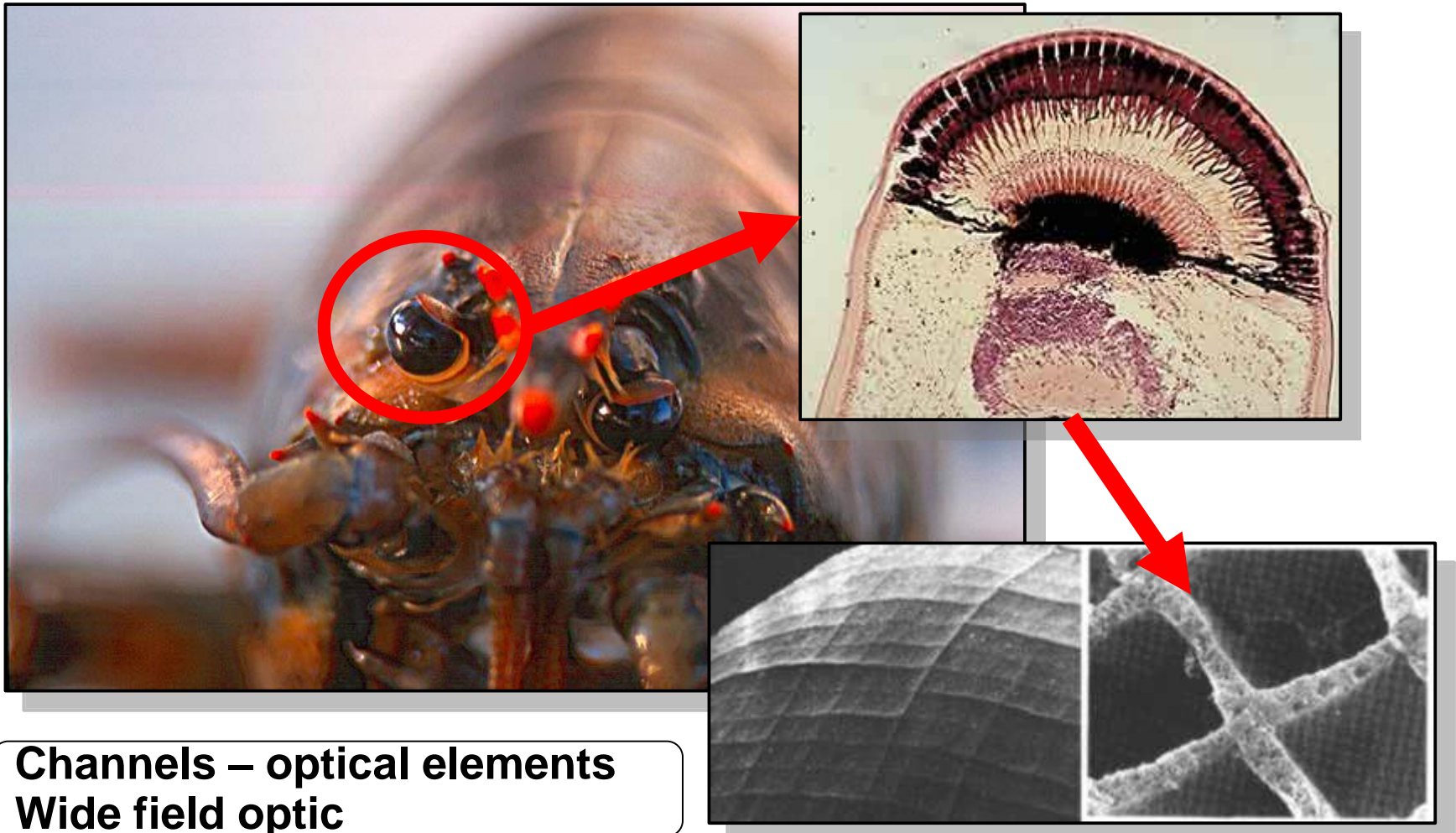
Multi Foil X-ray Optics (MFO)

- X-ray optics based on multiple thin X-ray foils
- Various foil materials
 - glass
 - Si
 - metal ...
- Various arrangements and geometries
 - Lobster Eye
 - KB system
 - Wolter
 - Double conical approximation to Wolter...

Motivation – wide field imaging

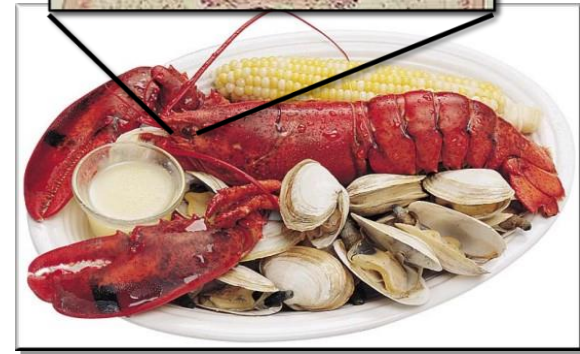
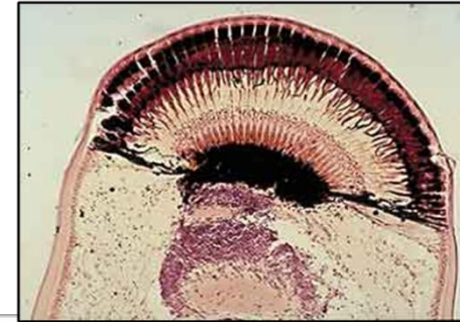
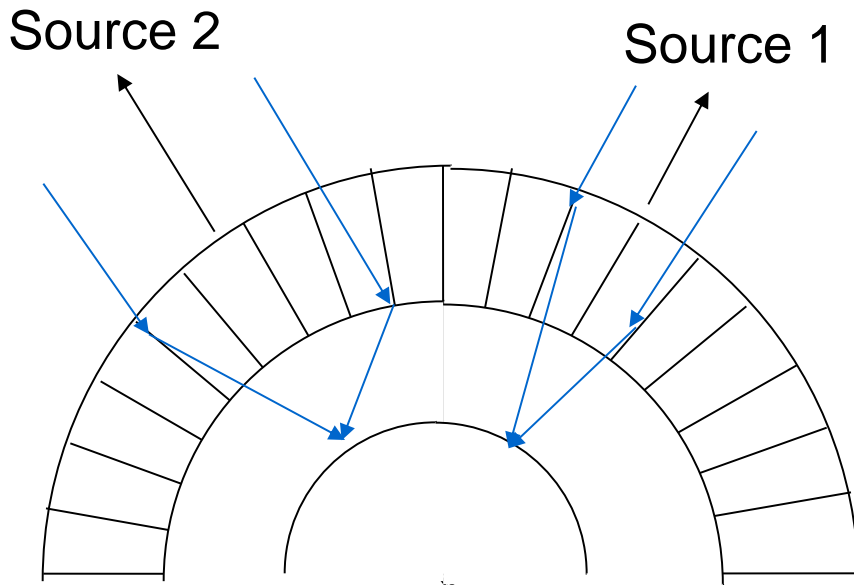
- Astronomical sources
 - Imaging
 - Image reconstruction
 - Scanning observations
- Laboratory sources
 - Imaging
 - Image reconstruction
- Other optic types

Lobster Eye



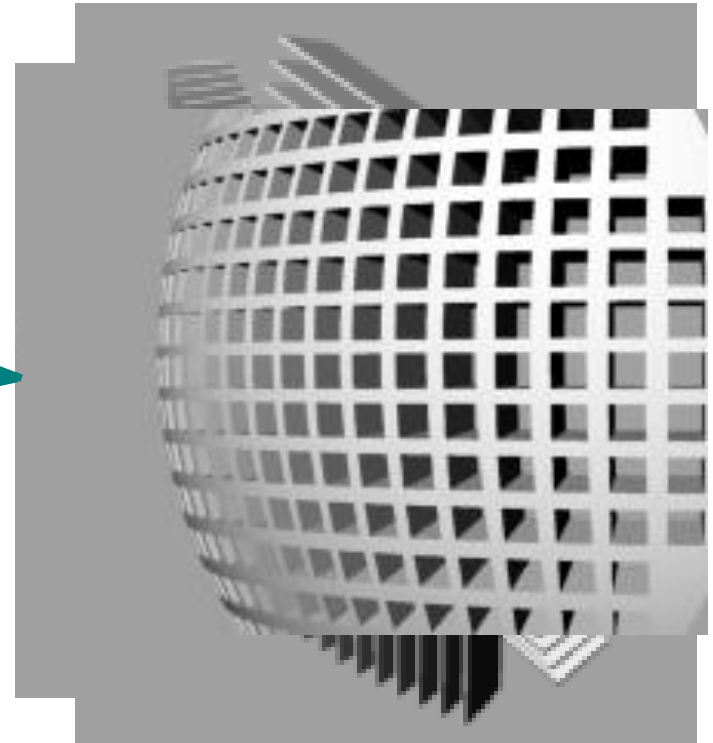
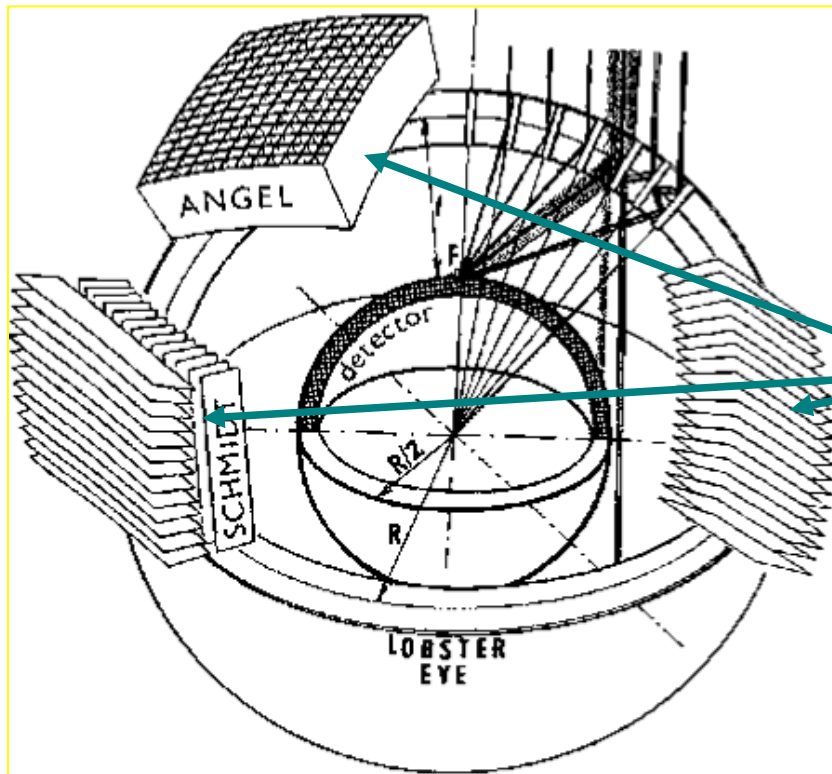
Channels – optical elements
Wide field optic

Lobster Eye (MFO) Geometry



- Reflection from two orthogonal stacks of planar mirrors (Schmidt)
- Wide field imaging
- LE modification - planar mirrors replaced by elliptical mirrors (MF KB, MFO)
- Focusing (no wide field feature)

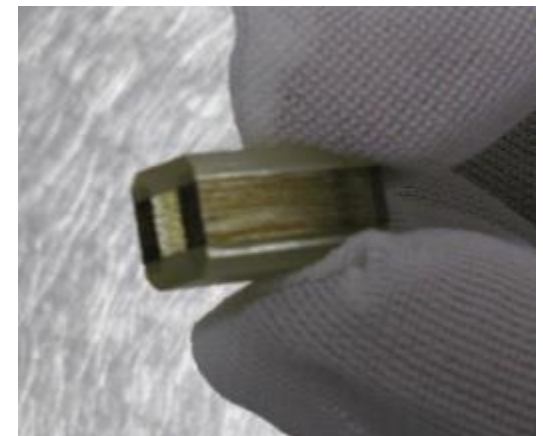
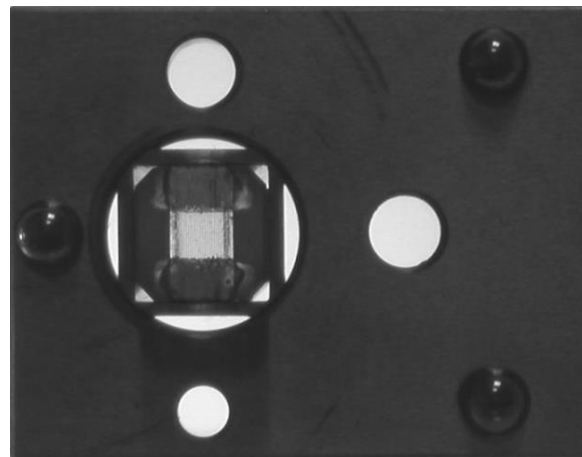
Lobster Eye (MFO) Optic Concept



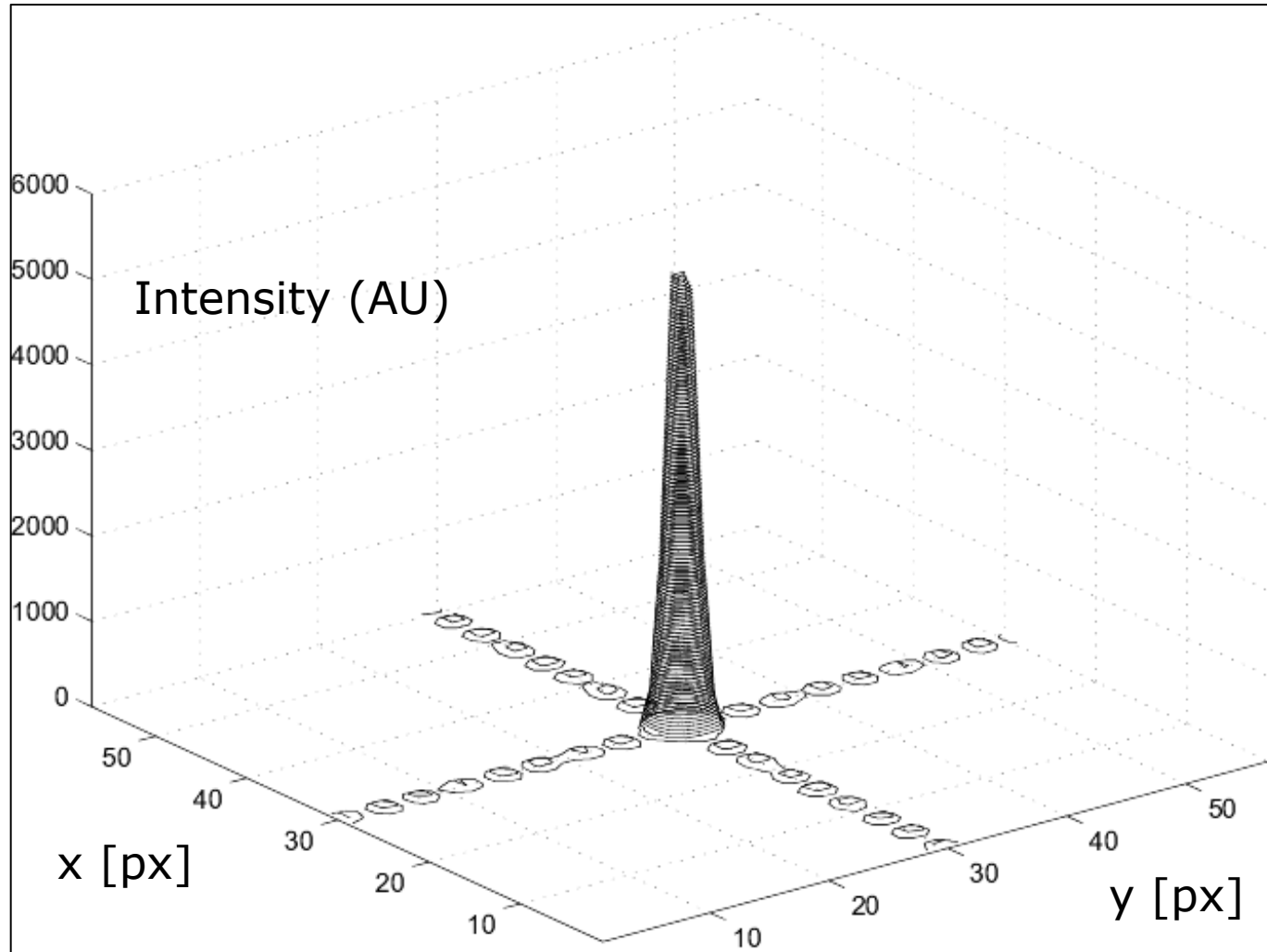
Multi-Foil X-ray Optics

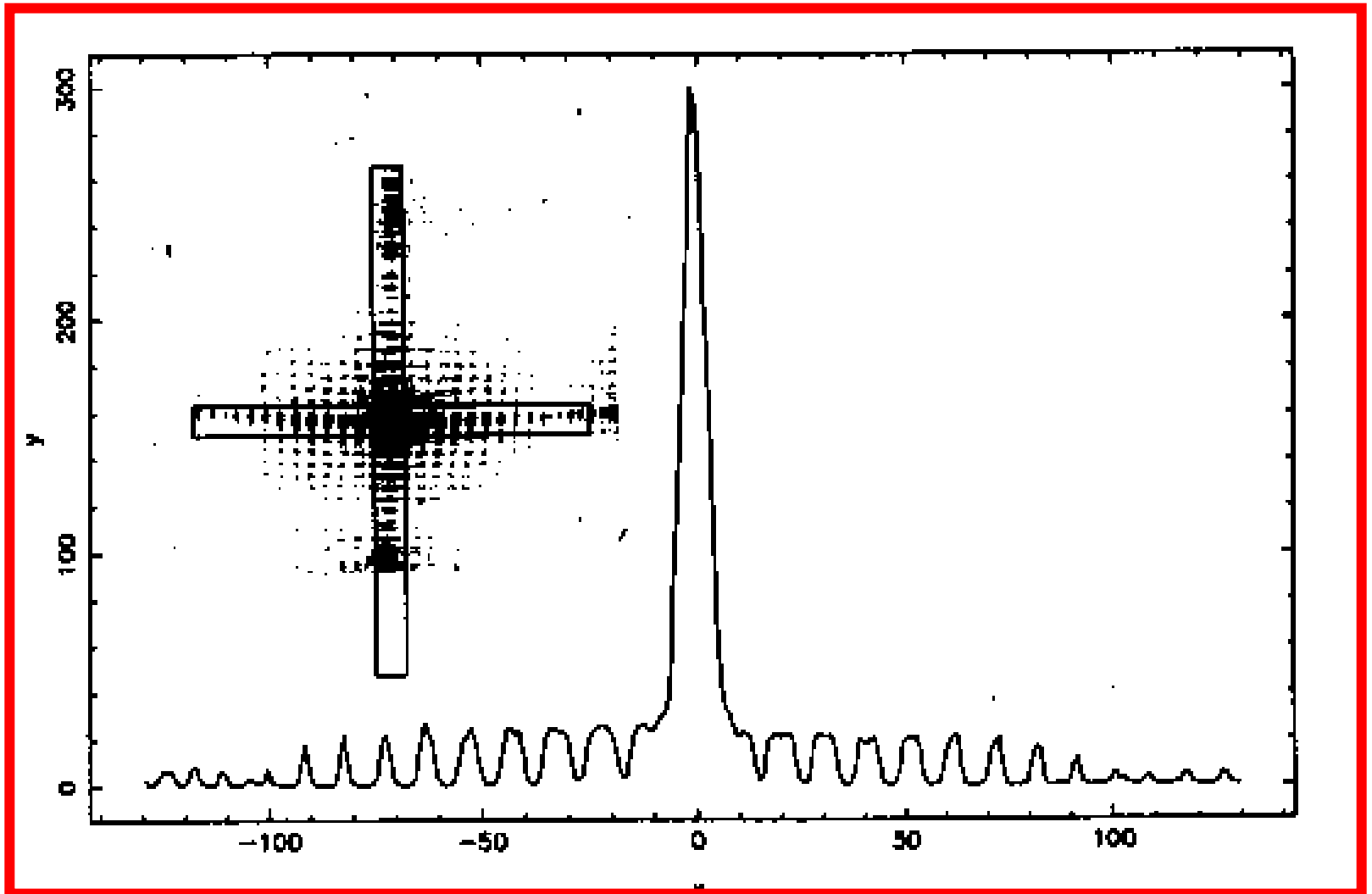
Various examples of Lobster Eye and MFOs

- foil thicknesses from 30 μm to 1 mm
- foils 3 x 3 mm to 300 x 300 mm
- planar & ellipsoidal



Single Point Imaging – Typical PSF

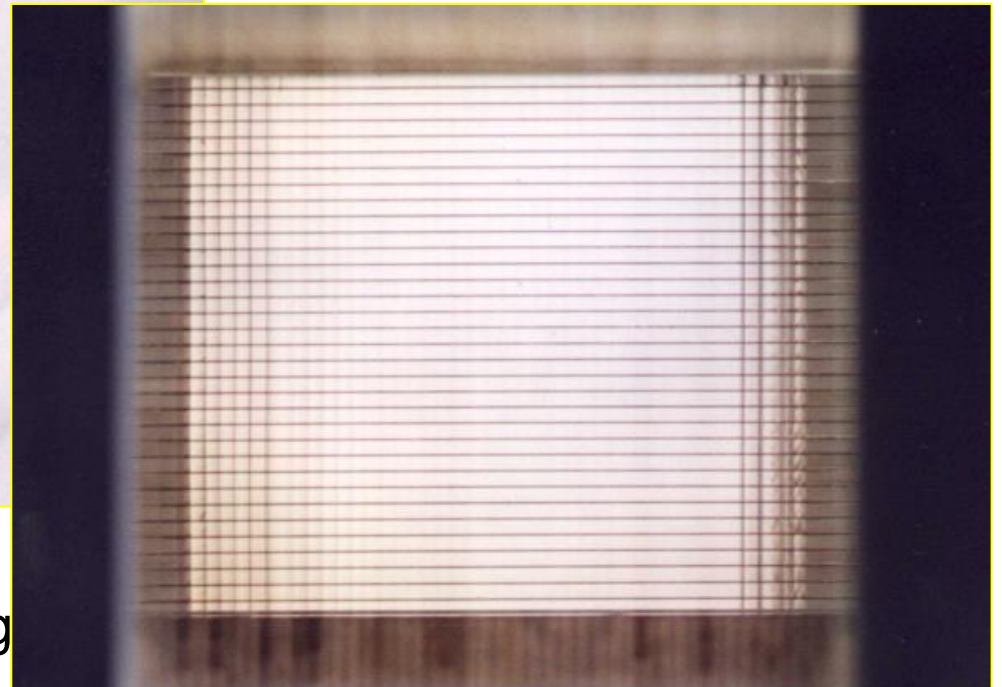
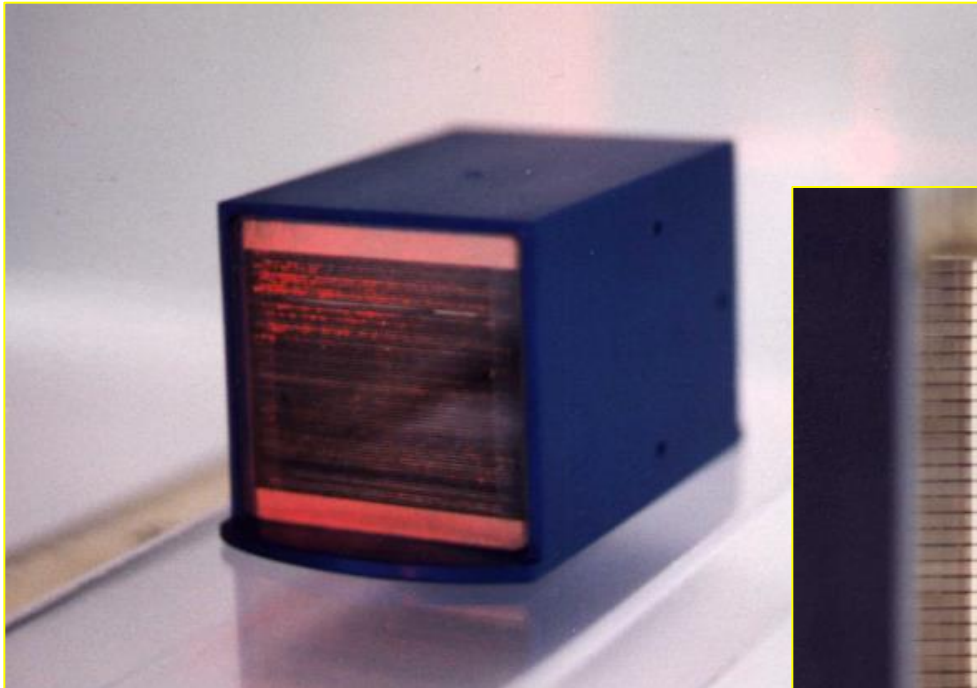




X - ray focal image of the 80 x 100 mm Schmidt prototype at 1.5 nm (X-ray test facility, University of Leicester, UK). The measured gain is 185

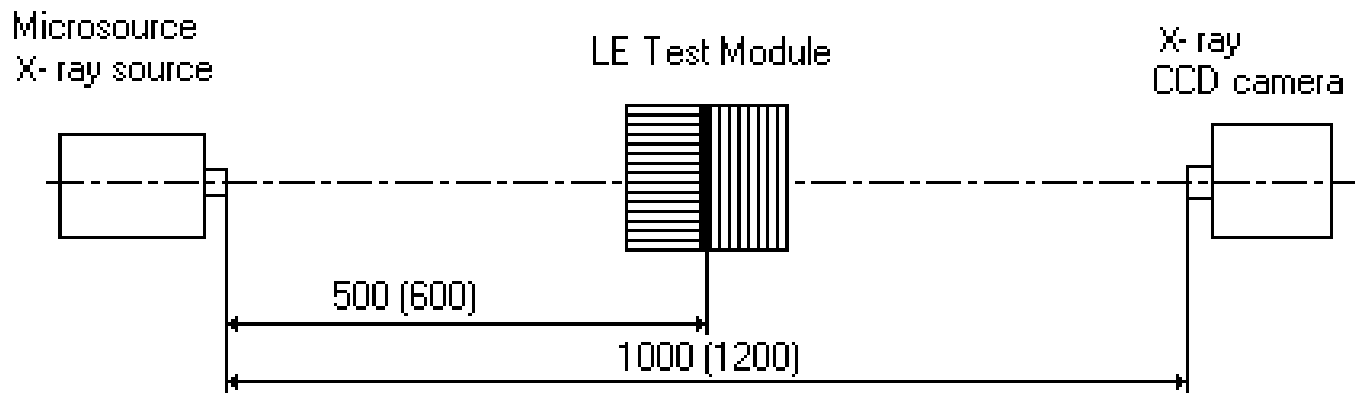
Multi-Foil X-ray Optic

- thin foils
- additional coatings
- shape variations

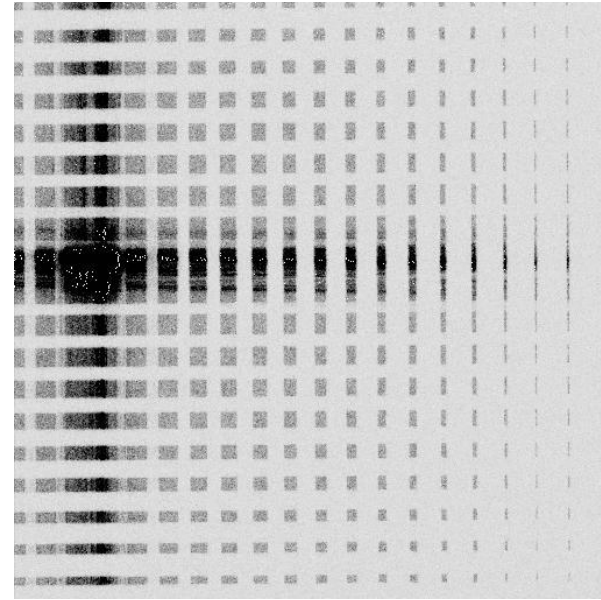
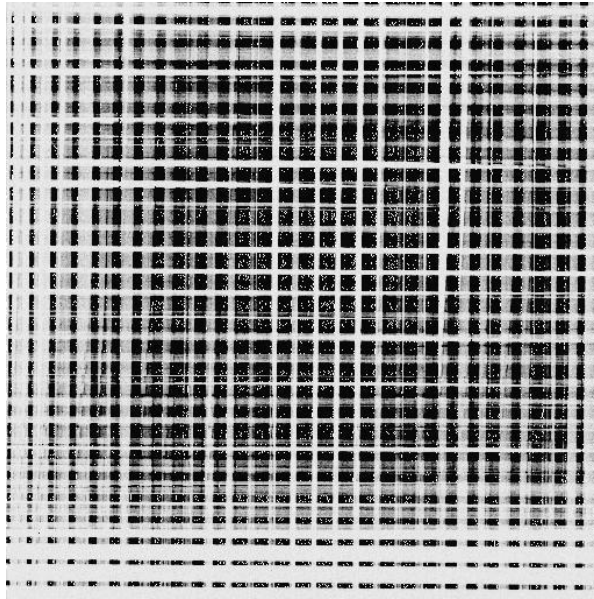


20 x 20 mm front area
100 μm thickness, 300 μm spacing

Experimental setup



Multi-Foil X-ray Optics

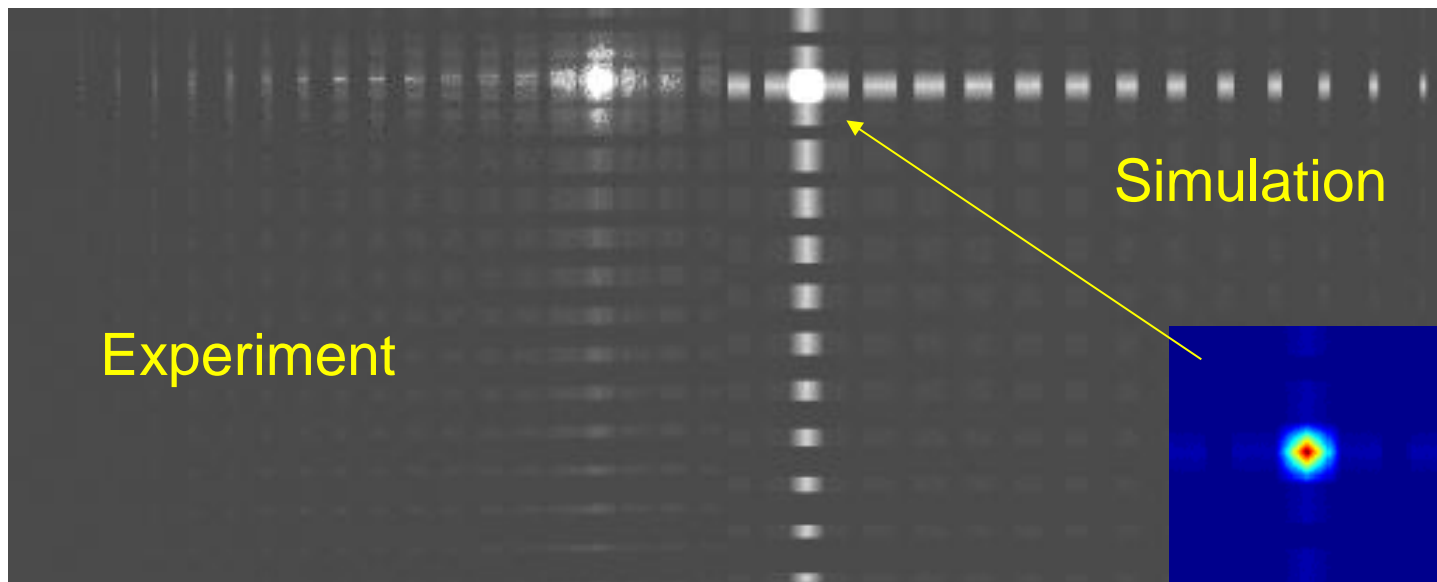


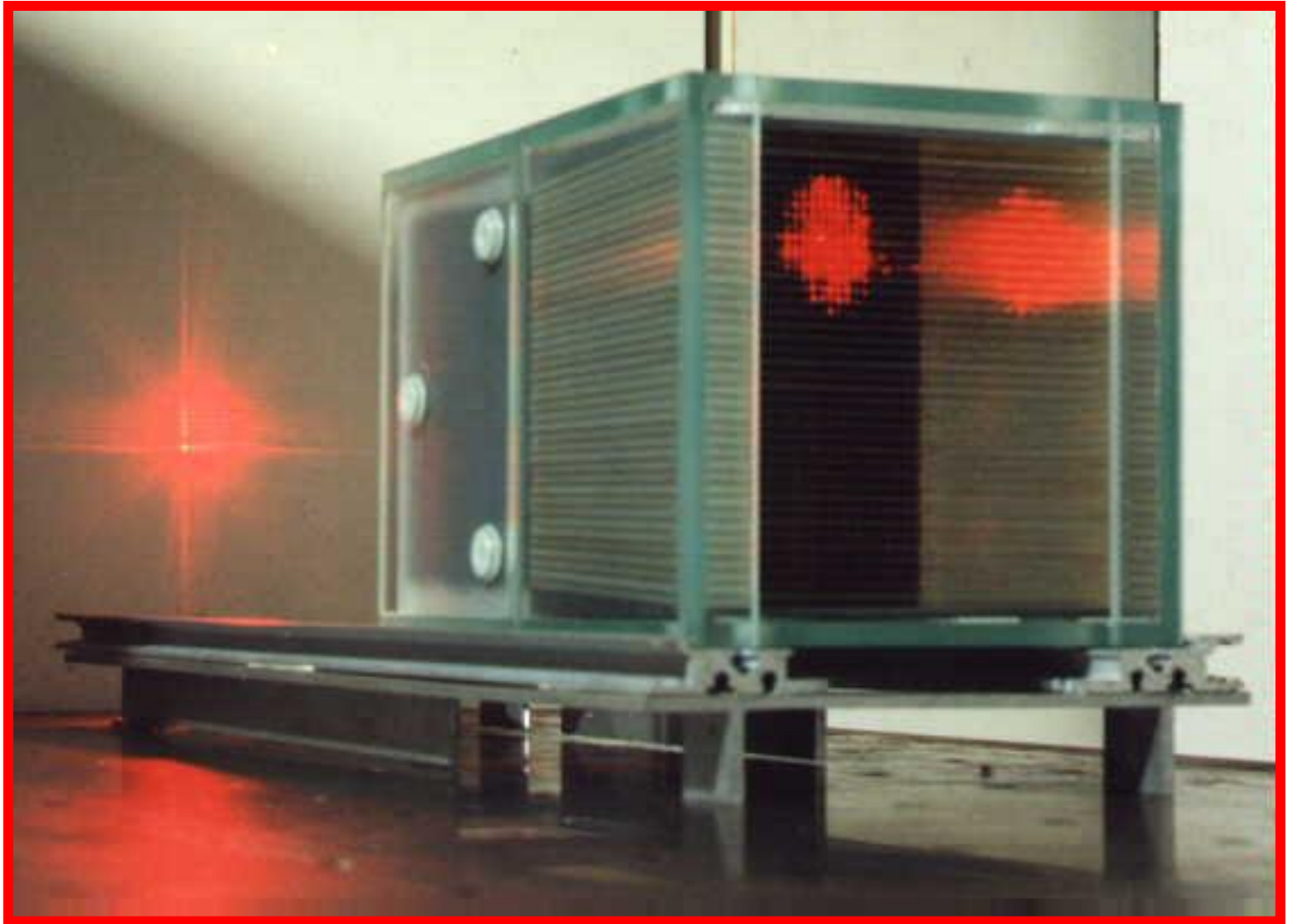
The X-ray shadowgram of the LES module showing the 100 micron thick gold plated flats and approx. 300 micron spaces separating them (and also confirming the high optical quality of used flats). Right: The X-ray focal spot image (LES module).

Multi-Foil X-ray Optics

LE X-ray experiment vs theory

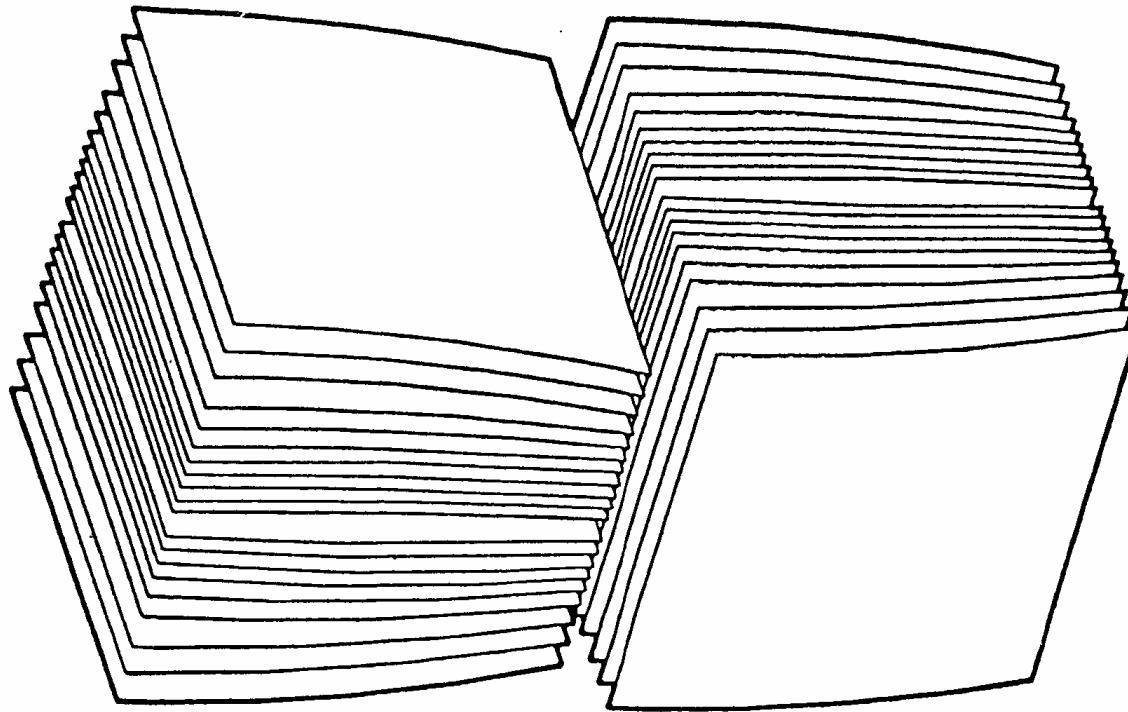
- Point-to-point focusing system
- Source: 20 μm size, 8 keV photons
- Source-detector distance: 1.2 m, 8 keV photons
- Detector: 512x512 pixels, 24x24 μm pixel size
- Gain: ~ 570 (experiment) vs. ~ 584 (comp. simulation)





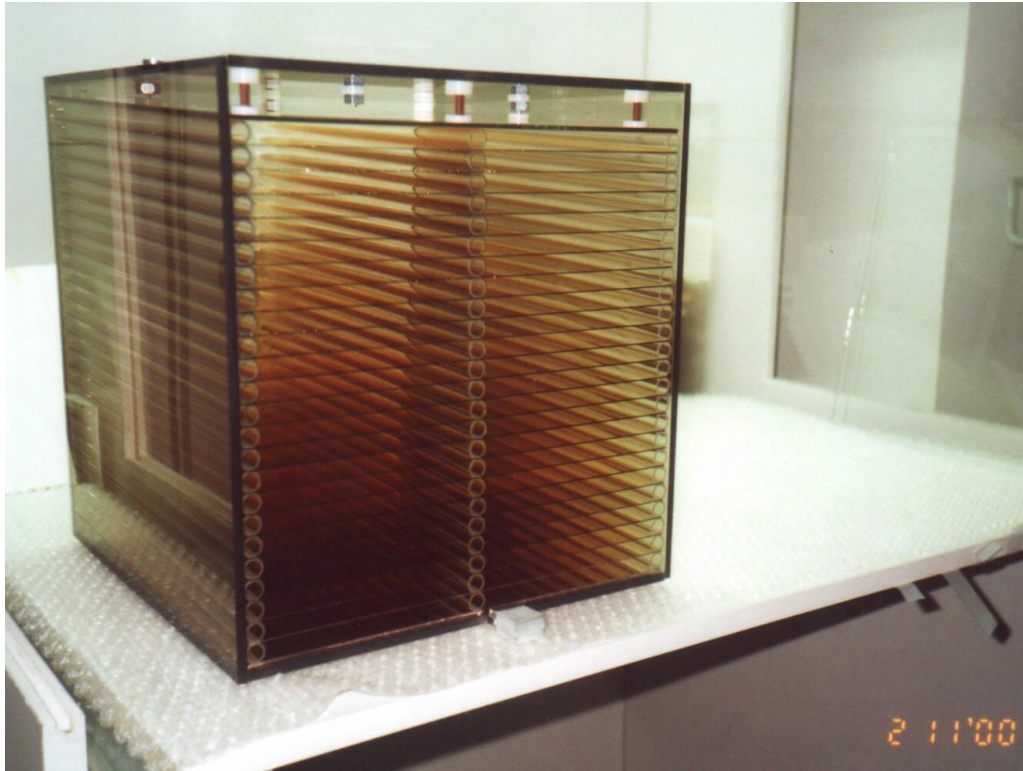
EXTATIC Prague, September 2017

Kirkpatrick-Baez Multi Foil X-ray Optic



Kirkpatrick-Baez mirror consisting of orthogonal stacks of reflectors. Each reflector a parabola in one dimension.

Kirkpatrick-Baez Multi Foil X-ray Optic



XEUS test mirror assembly

2D module,

30 x 30 cm glass foils

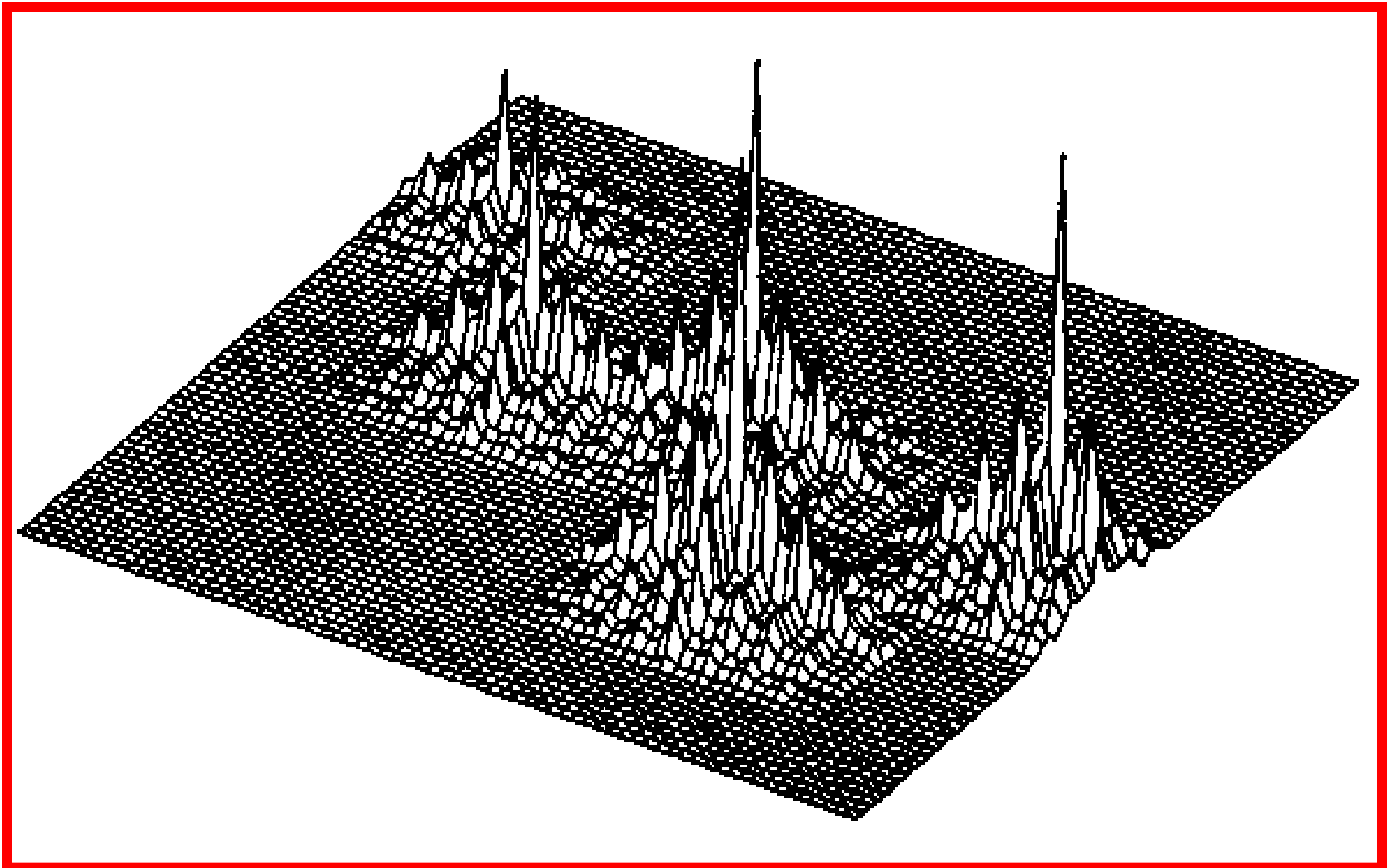
0.75 mm thickness of foils

gold-coated by sputtering,

plates spaced at 12 mm.

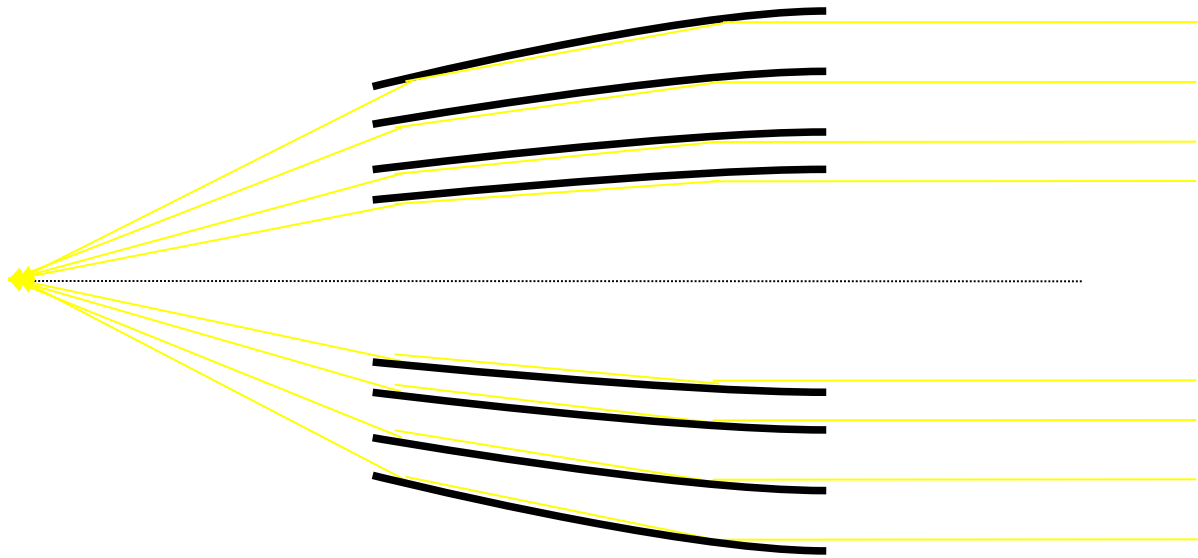
Tests of LE modules, XEUS
modules, large K-B modules.

Light-weight (glass)



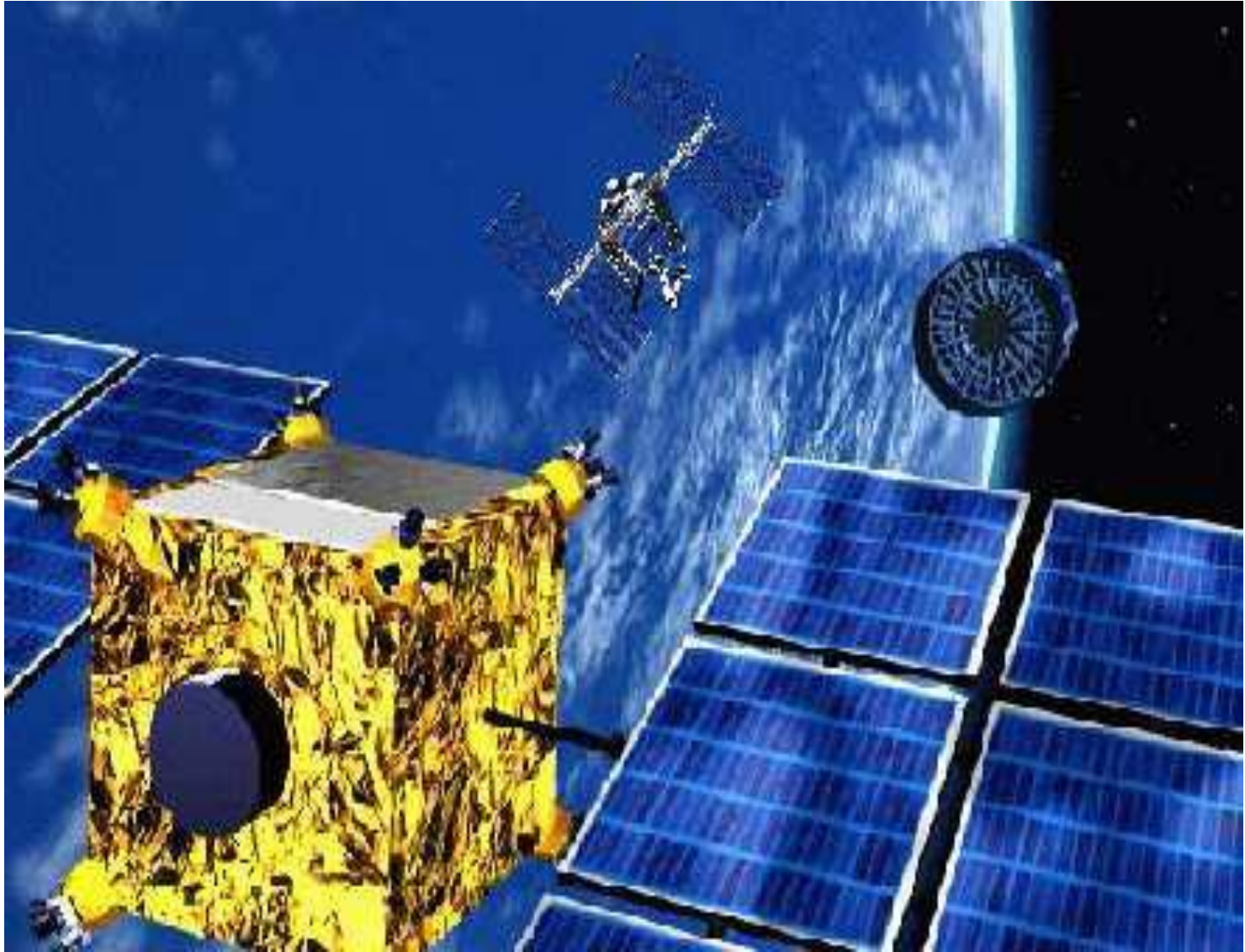
The Cassiopea constellation as seen by the Angel type Lobster - eye telescope (computer ray - tracing)

Typical X-Ray Telescope

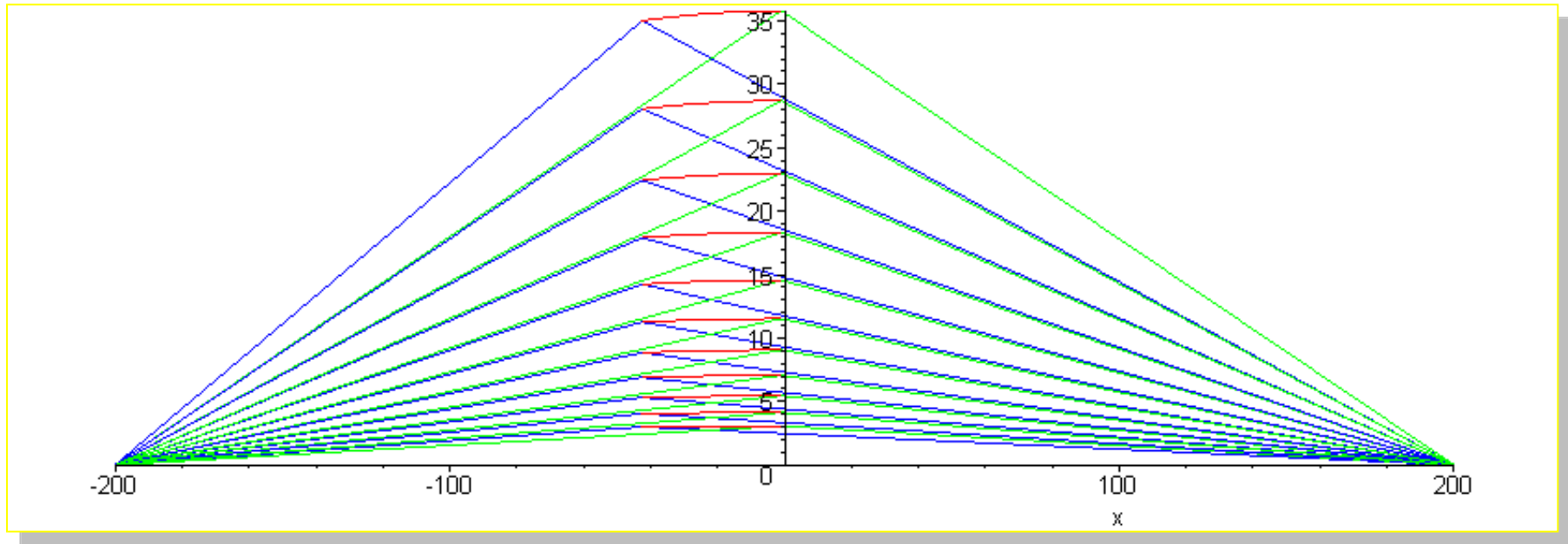






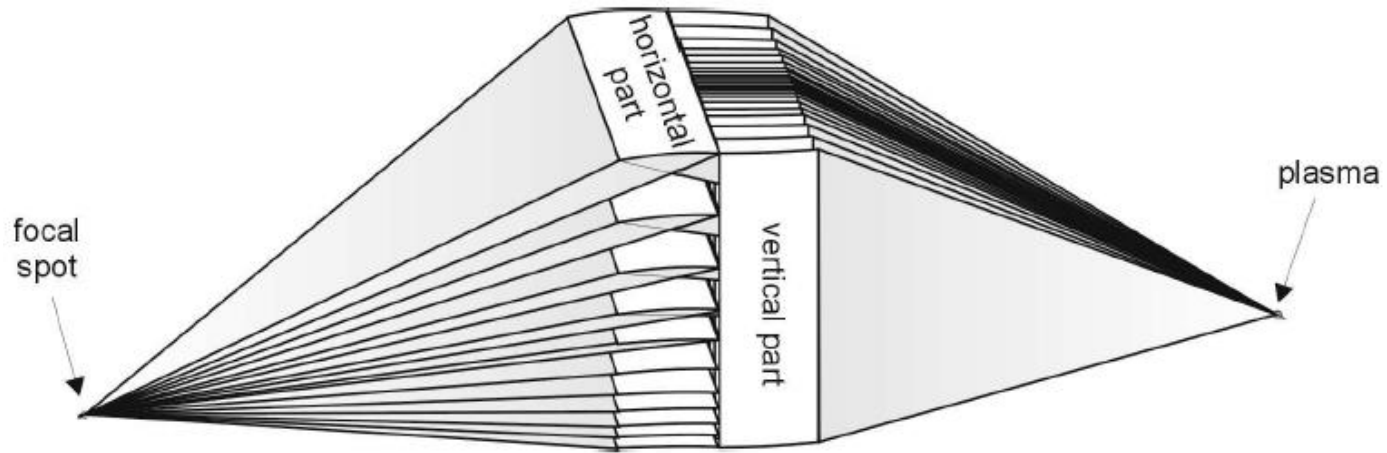


MFO EUV condensor



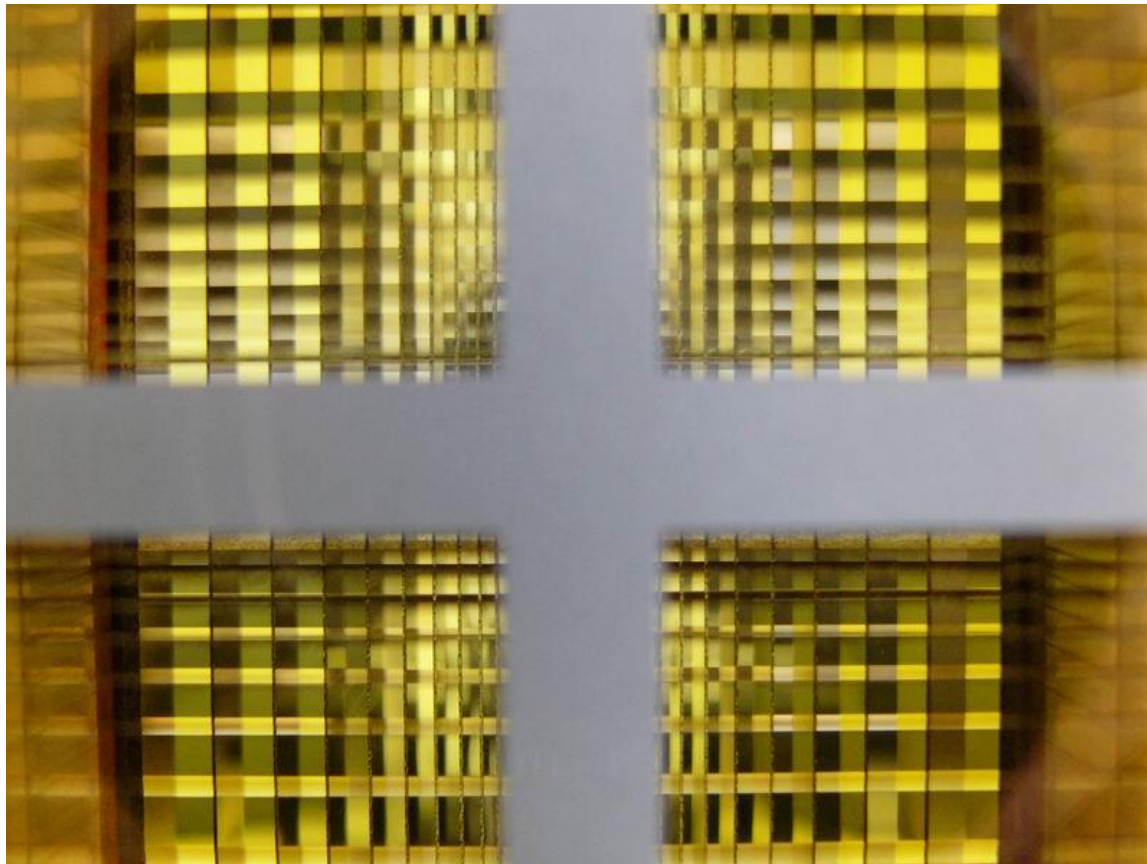
Optic profile – a quarter of the optic system is displayed, all dimensions in millimeters. Ellipsoidal mirrors, length 40mm, width 80mm.

MFO EUV condensor

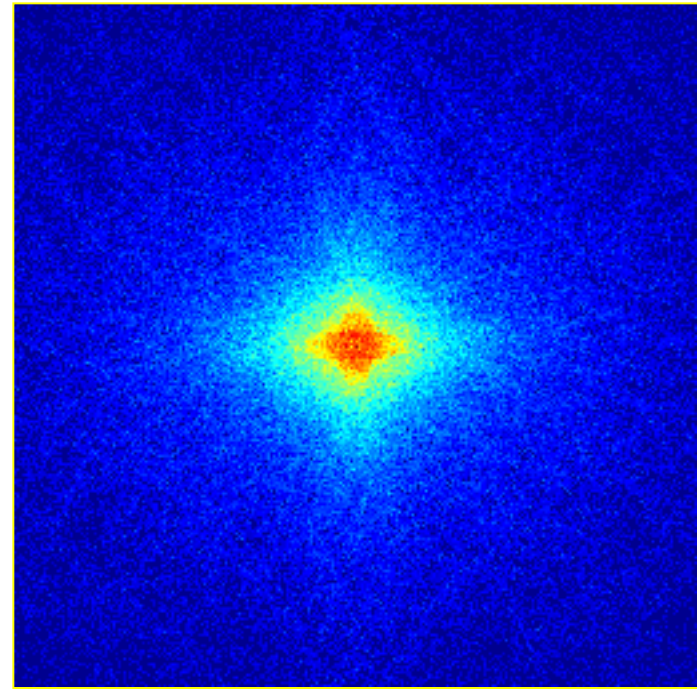
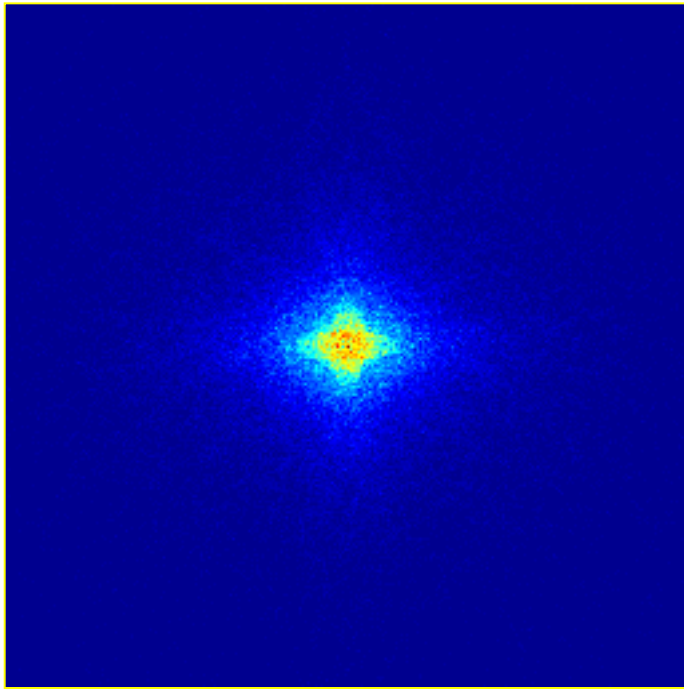


Experimental setup of MFO condenser

Two orthogonal sets of elliptical mirrors

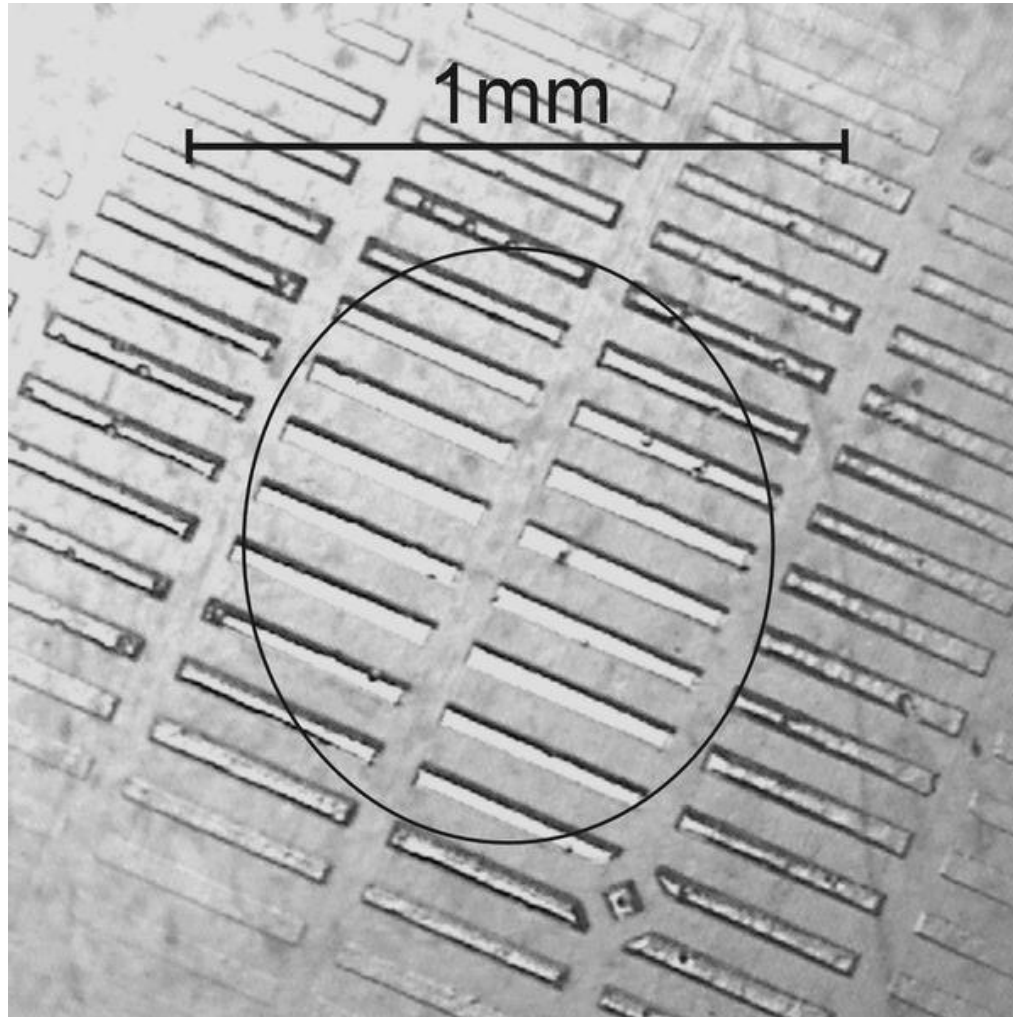


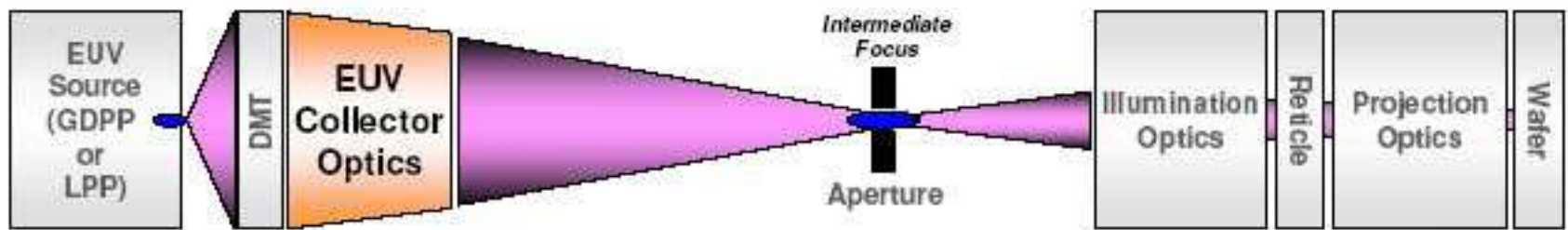
Ray-tracing for point source



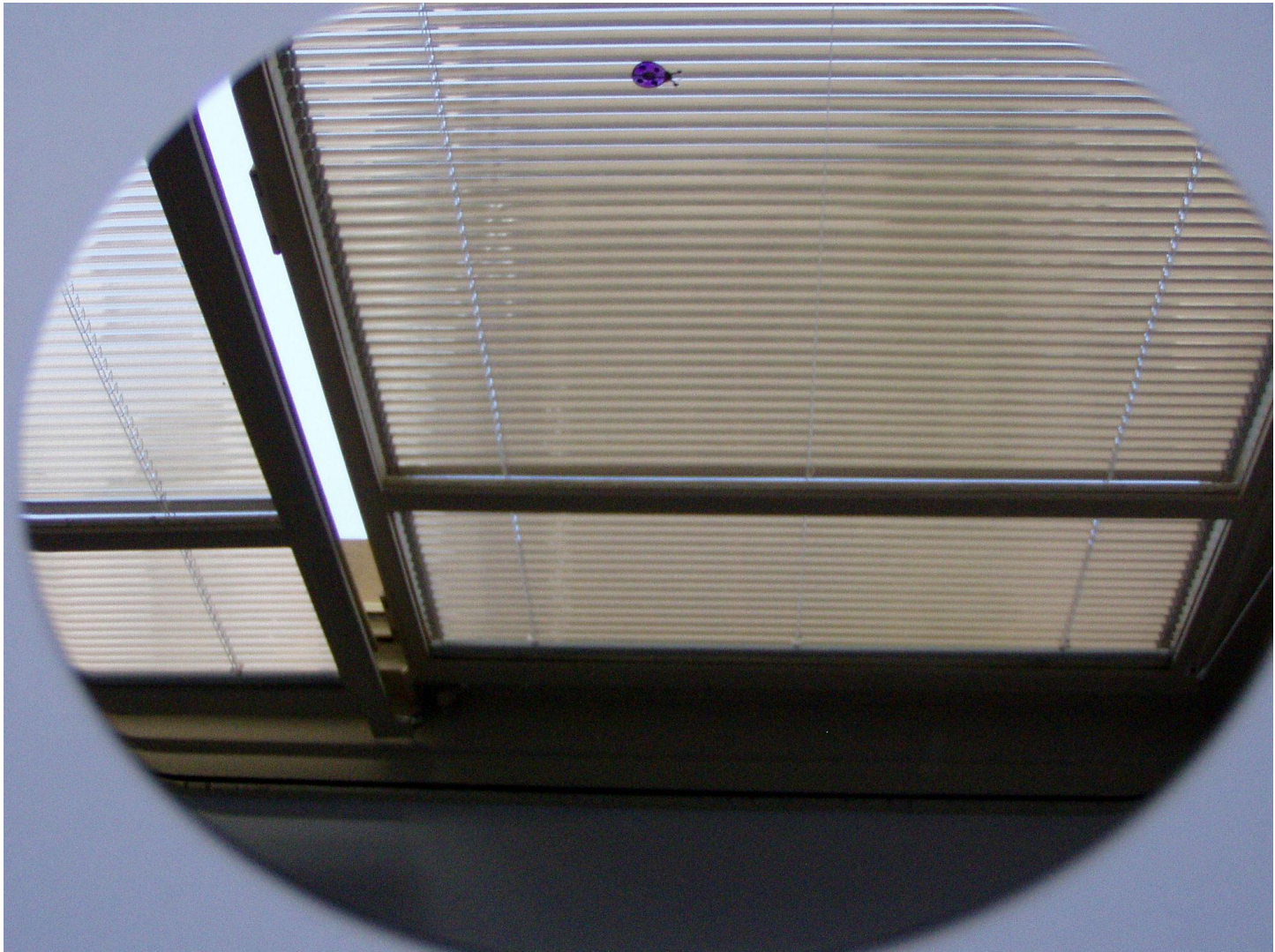
Focal spot for point source, $1\mu\text{m}$ pixel size, 256×256 pixels each.
Linear intensity scale on the left, $\sqrt{\text{intensity}}$ intensity scale on the right

TEFLON layer exposed by EUV radiation



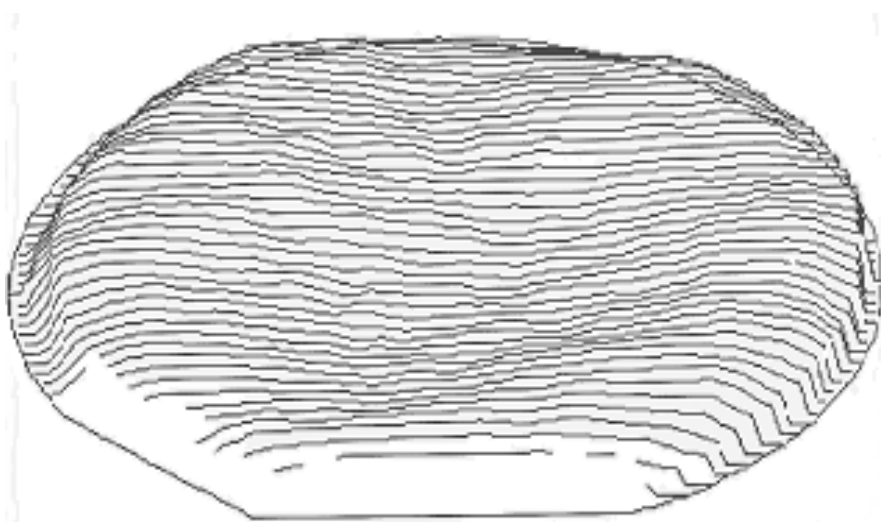


X-RAY OPTICS BASED ON Si WAFERS



Slightly parabolized $D = 150$ mm Si wafer
(ON Semiconductor Czech Republic)

Flatness measurements of Si wafer produced by ON Semiconductor Czech Republic

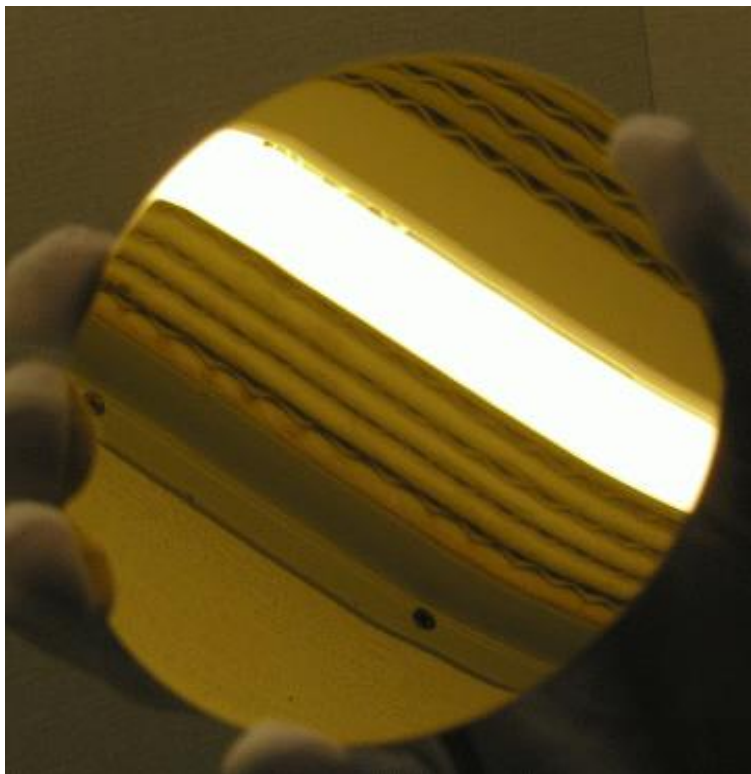


min. thickness	686.07 μm
max. thickness	687.75 μm
ave. thickness	687.18 μm
cen. thickness	686.92 μm
TTV Total Thickness Variation	1.68 μm
TIR Total Indicated Reading	1.81 μm

Flatness and thickness uniformity of a Si wafer (diameter 150 mm)

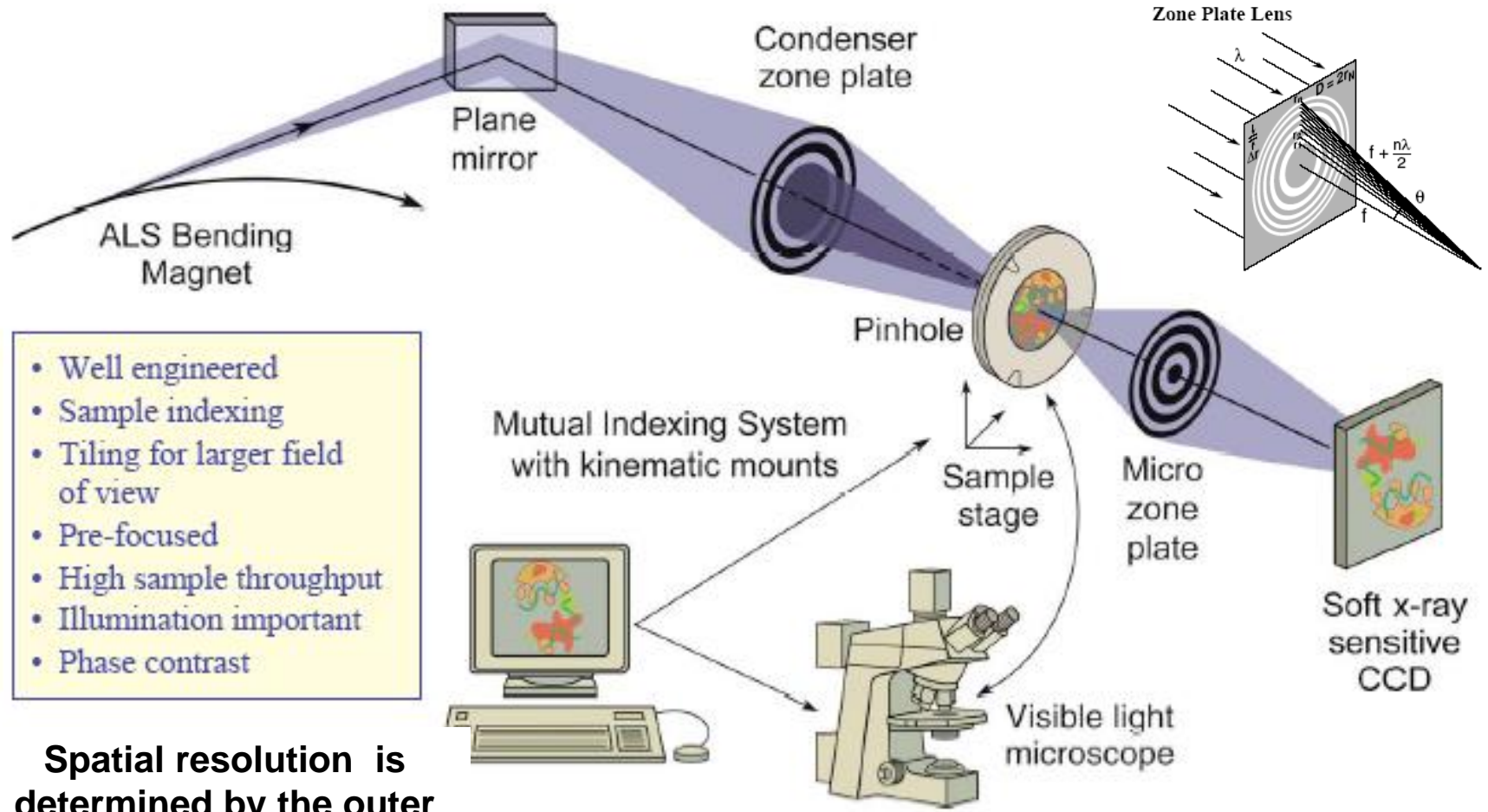
Si WAFERS SHAPING

test cylindrical samples
gold-coated, $d=100$ mm, thickness 0.8 mm, $R=1.3$ m



XR/XUV Micron to Submicron Resolution Laboratory Microscopy and μ CT

X-ray Microscope based on a Fresnel optics



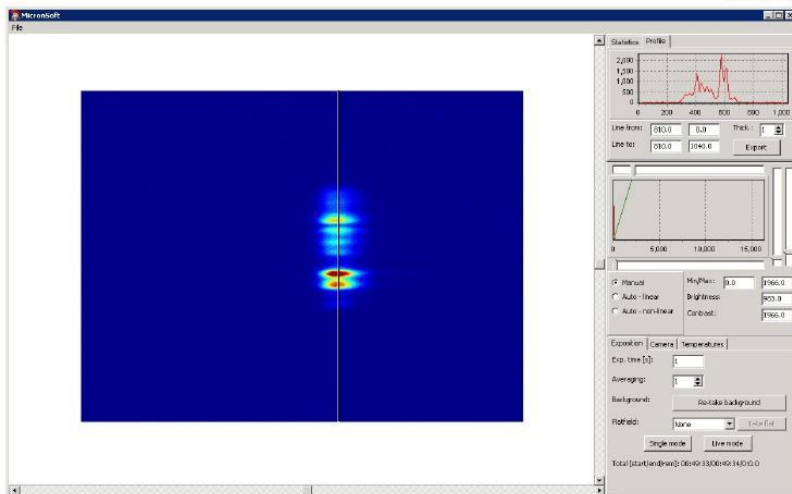
- Well engineered
- Sample indexing
- Tiling for larger field of view
- Pre-focused
- High sample throughput
- Illumination important
- Phase contrast

Spatial resolution is determined by the outer zone width $\Delta r \sim 15\text{-}50\text{nm}$

Xsight™ Micron X-ray CCD Camera

Applications:

- X-ray microscopy
- X-ray microtomography
- X-ray optics adjustment & metrology
- Phase contrast X-ray imaging

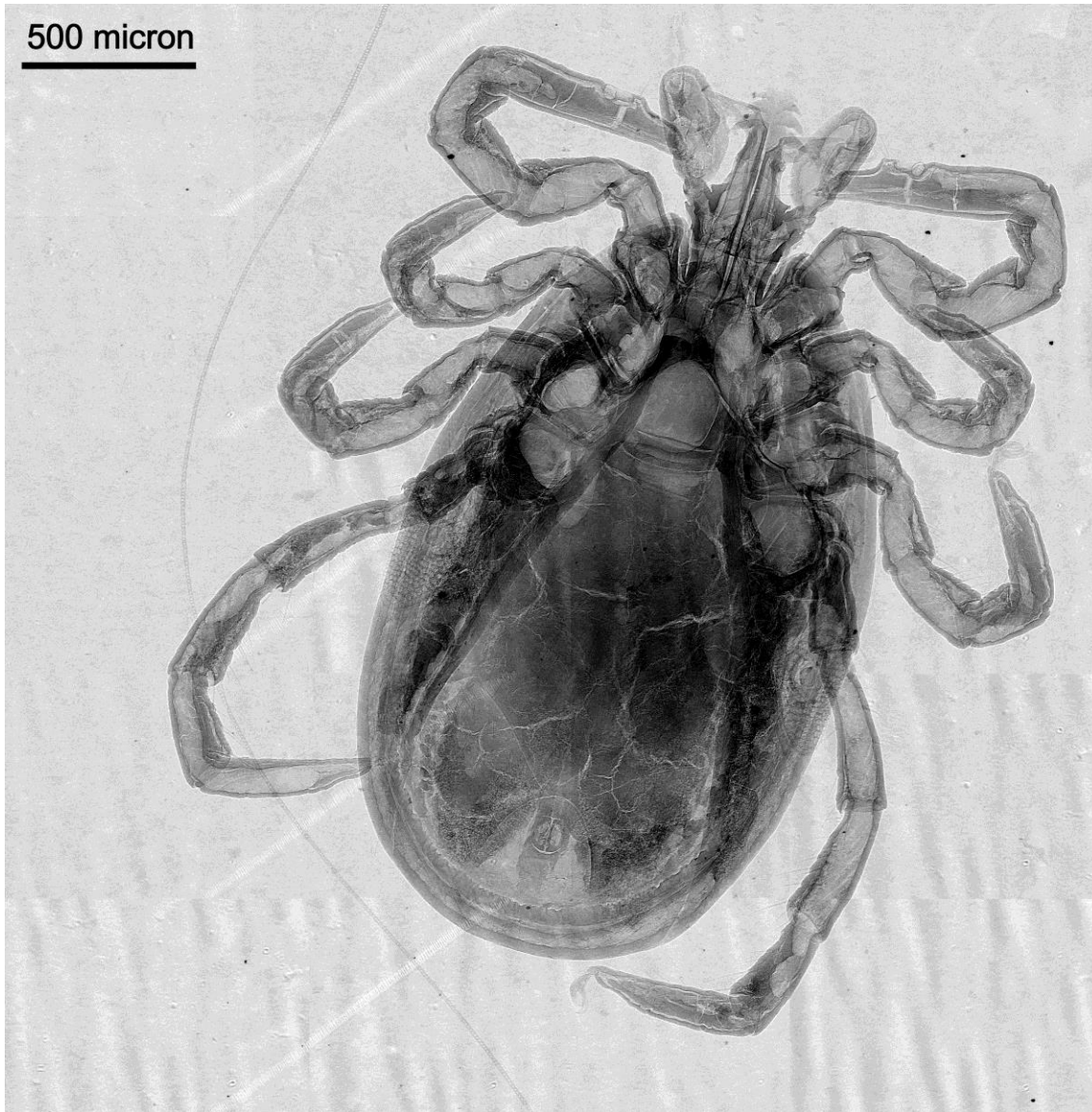


Field of view: 0,90 mm x 0,67 mm
Resolution: $\leq 1 \mu\text{m}$ (@ 8 keV)
Spectral range: 50 eV to 35 keV
Exposure time range: 20 μs to 500 s
Dynamic range: 70 dB
Dimensions: 60 x 70 x 250
Weight: 2.5 kg

Projection X-ray Microscopy
RITE and CTU, microfocuss X-ray tube 8 keV (Prague, Czech Republic)



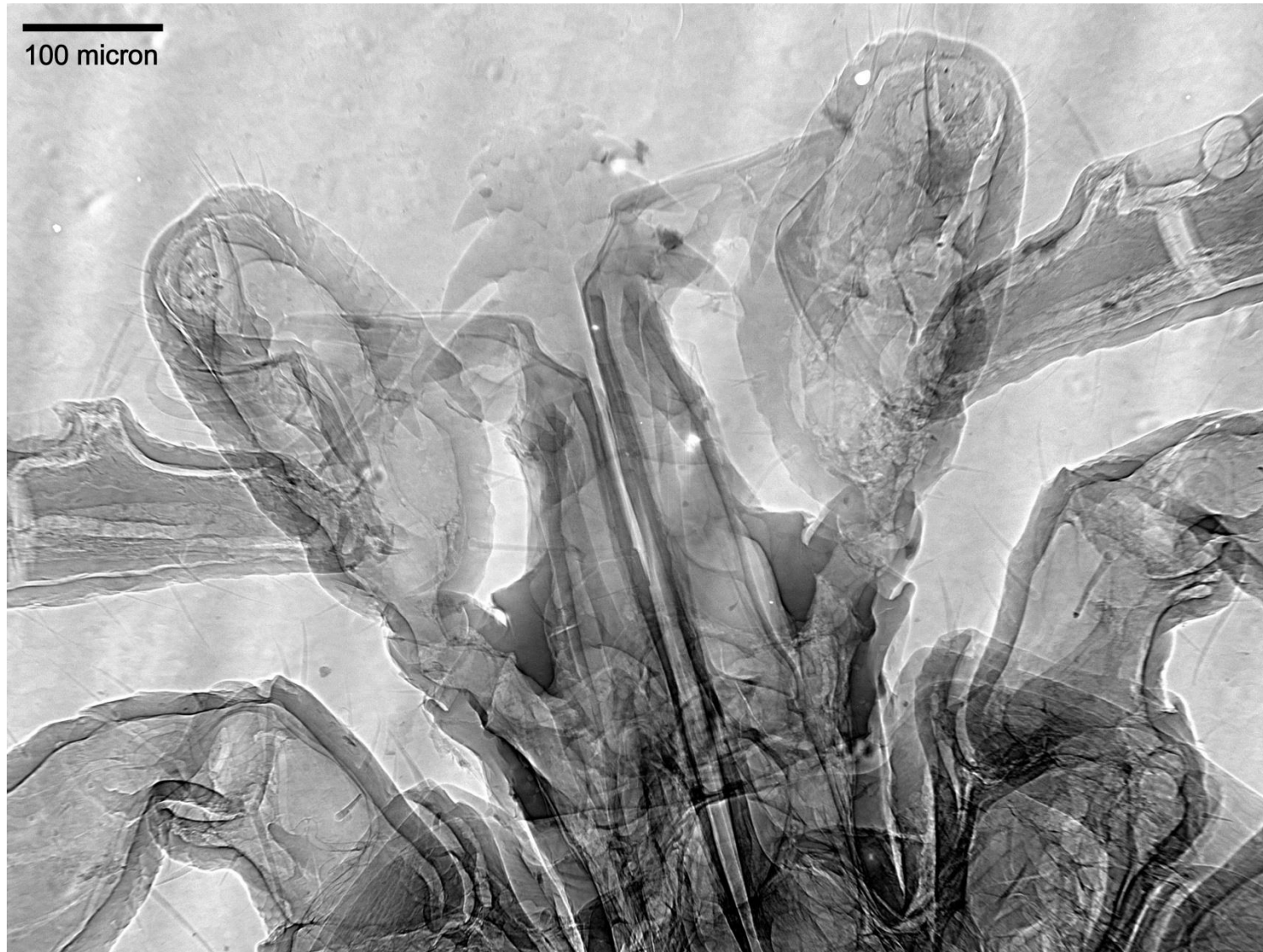
Projection X-ray Microscopy



X-ray image of *Ixodes Ricinus*

(Taken by XSight Micron at RITE laboratory using
80 W microfocus X-ray tube with Cu target)

Projection X-ray Microscopy

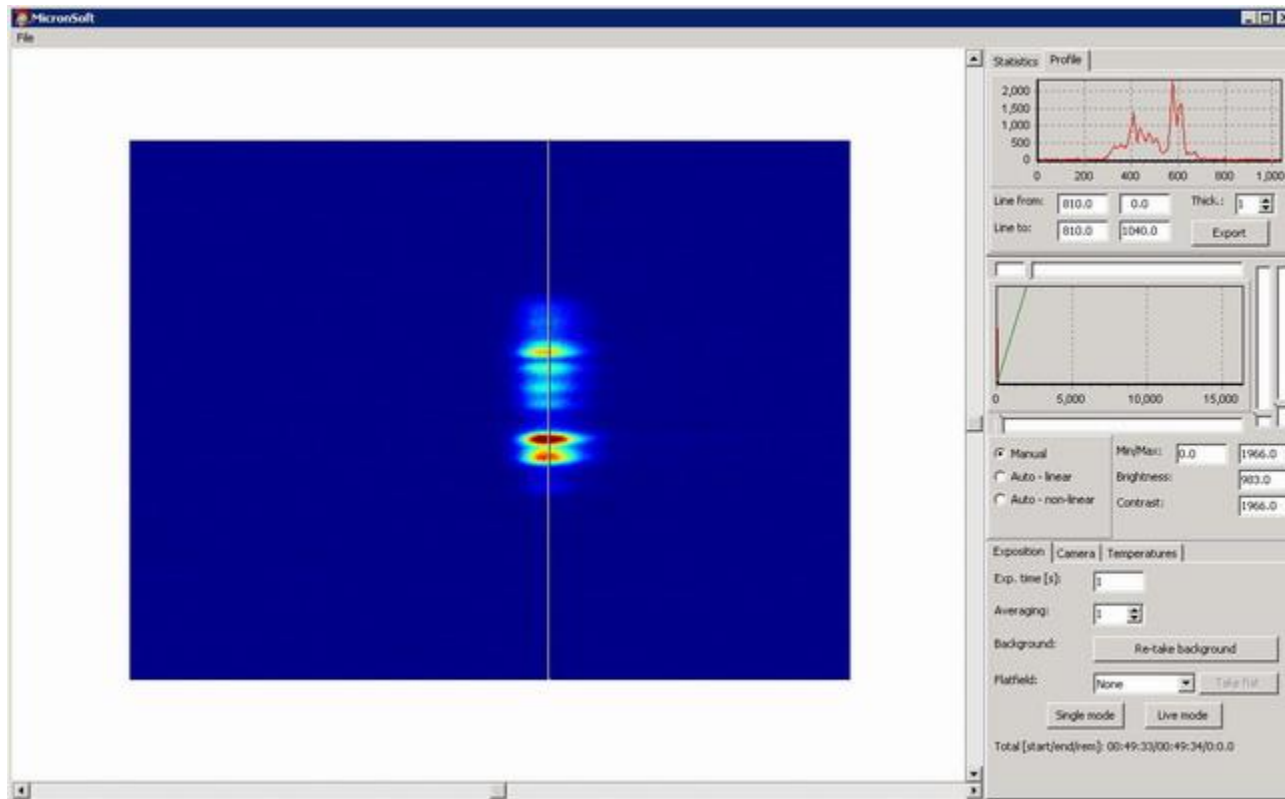


X-ray image of *Ixodes Ricinus*

(Taken by XSight Micron at RITE laboratory using 80 W microfocus X-ray tube with Cu target)

Projection X-ray Microscopy

Advanced Photon Source synchrotron facility (USA)



„Image of non-focused X-ray beam reflected by a bimorph mirror at beamline 21ID of the Advanced Photon Source. Separate peaks correspond to reflections by the mirror segments“, by courtesy of Dr. Elena Kondrashkina, Synchrotron Research/LS-CAT, Northwestern University. RITE Xsight Micron camera, pixel size 0.65 μm

Ultra High Resolution 3D X-ray Tomography

POWER : Ultra High flux, up to 1200 W

ENERGY: Cr, Cu , Mo

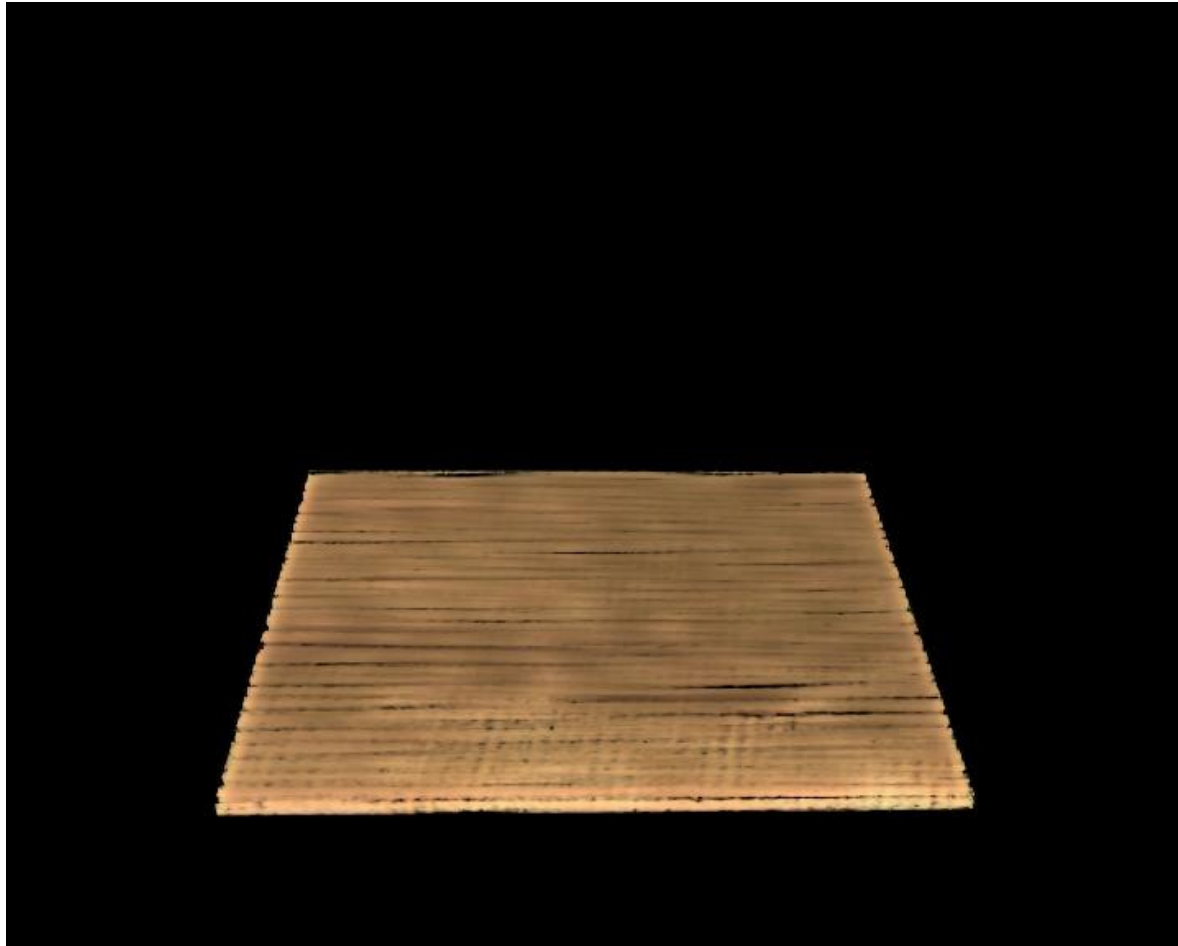
DETECTOR: 3300 x 3300 x 2500 Matrix

OPTICS: No projection magnification

EASY: Minimal Alignment or optimisation



High Contrast X-ray Imaging and Tomography of Material Samples



CFRP
0.27 μ m voxel
3200 x 3200 x 2500 (0.9mm)
Cu Anode 8keV

RES
FOV:
ENERGY:

6 μ m Carbon Fibres

THANK YOU FOR ATTENTION



Prague

